

Quarterly Report

Date of Report: October 1, 2009
Contract Number: DTPH56-08-T-000008
Prepared for: DOT
Project Title: Achieving Maximum Crack Remediation Effect from Optimized Hydrotesting
Prepared by: Dr. Weixing Chen
Department of Chemical and Materials Engineering
University of Alberta
Edmonton, Canada
Tel: 780-492-7706
Email: Weixing.Chen@ualberta.ca

(For quarterly period ending: September 30, 2009)

Task #	ACTIVITY or DELIVERABLE	SCH Date	CMPL Date
2.3	Operation model	05/01/2009	08/31/2009
2.4	Cracking stage correction model	08/01/2009	11/30/2009
6	5th Quarterly Status Report	07/1/2009	09/30/2009

- Technical Status – description of tasks completed, data from test results, Graphs, charts, tables of technical importance, photos of items under investigation, research findings and/or discoveries.

Project activities undertaken through the 5th quarter focused on 1) operational conditions that will change the morphology at the crack tip (sharp or blunt) and their effect on crack growth during hydrostatic loading; 2) crack growth rate as affected by crack dimensions and crack aspect ratios.

On the effect of operation conditions-dependence of crack growth on crack tip morphology and hydrogen effects: One important progress made in this period is the publication of a journal article entitled “Transgranular Crack Growth in the Pipeline Steels Exposed to Near-neutral pH Soil Aqueous Solutions-Role of Hydrogen”, Acta Mater, doi:10.1016/j.actamat.2009.08.047. In the paper, we have clearly defined the controlling factors and their role played in the entire process of crack initiation and propagation towards the final failure of steel pipelines in the field. It has been found based on experimental results that near-neutral pH cracking results from the following two competitive processes at the crack tip:

Crack tip blunting: originates from low temperature creep deformation due to near-static loading (situation of SCC) and slow loading rate (situation of fatigue at very low frequency), and the active dissolution over the deformed crack tip without producing passivation.

Crack tip sharpening: occurs concurrently or sequentially with the process of crack tip blunting and is related to the process of cyclic loading and the hydrogen effects.

The balance between crack tip blunting and sharpening determines if cracks will experience dormancy or active growth. This unique balance depends on the type of loading and the stage of cracking. Under static loading (scenario of stress corrosion cracking), crack tip blunting is more likely, resulting in mostly dormant cracks. When cracks are subjected to cyclic loading (a situation of corrosion fatigue), the blunting process is attenuated but the sharpening process is enhanced such that the two processes can be very competitive, depending on the environments, cathodic protection and pressure fluctuations. Since pipelines, particularly those for high pressure gas transmission are operated under a near static condition most of time, crack growth proceeds normally by repeated cycles of dormancy and active growth with a growth rate substantially higher than generally estimated in the field.

For a given pipeline system, the presence of near neutral pH environments and high residual stresses on the pipe surface determines whether a crack colony can be developed, while the presence of high concentration of diffusible hydrogen is thought to determine whether repeated crack growth is possible to occur. Hydrogen produced by corrosion at the crack tip is secondary in terms of crack growth, as compared with the amount of hydrogen generated from pipeline surface either resulted from general corrosion or cathodic reaction. In order to observe a full effect of hydrogen, the test duration must be long enough to allow diffusible hydrogen generated on the specimen surface to reach an equilibrium state throughout the specimen. For example, a minimum of 275 hour exposure is needed for a specimen with a thickness of 9 mm, which was observed experimentally and is consistent with calculations based on diffusion laws.

8 hydrostatic simulations have been completed in this quarter. These tests were designed to consider the effect of operation conditions in terms of crack tip morphologies and the effect of diffusible hydrogen in the steel. Crack tip morphology was altered through room temperature creep or corrosion exposure under constant load prior to hydrostatic loading. The amount of diffusible hydrogen in the specimen was controlled by changing the time of exposure or by coating the sample surface to avoid the ingress of hydrogen prior to hydrostatic loading. The samples were also loaded to achieve different stress intensity factor representing different sizes of cracks in the pipeline steels. The samples after testing are currently under evaluation to determine the actual crack growth.

On the growth behavior of surface cracks: In this quarter, we have successfully completed two long term crack growth simulations using a long specimen (about 40 cm) containing multiple surface cracks. They were made by electro-discharge machining and pre-fatigued individually in air to produce a sharp crack tip prior to crack growth in near neutral pH environments. Special test cells were also designed such that the surface cracks can be exposed to different region of disbonded coatings cathodically protected at the opening mouth of the disbondment. The specimens after testing are currently under evaluation to determine the crack growth rate and the morphology of the cracks after growth.

- Business Status – summarize details of the resource status of this Agreement, including the status of the contributions by the Team Participants. Include a quarterly accounting (broken out by Project milestones) of budgeted, current and cumulative expenditures, including cost share amounts. Explain any major deviations and discuss the adjustment actions proposed. Describe discussions with operators, or potential users of technology under investigation.

We have conducted the project according to the original plans. We have obtained additional funding to support the project. Details of business status are given in the table below:

Business Status Section										
Item #	Task #	Activity/ Deliverable	Qtr #	Projected			Actual	Status of Cost-sharing	Major Deviations	Adjustment actions proposed
				Fed Pmt	Partner Cost-sharing	Total				
14	2.3	Operation model	5	10,000	3,000	13,000	25,000	15,000	12,000	cash paid by partners*
15	2.4	Cracking stage corrosion model	5	5,000	13,000	18,000	28000	23,000	10,000	cash paid by partners
16	6	5th 1/4ly status	5	2,500	1,000	3,500	3,500	1,000	0	

* Partners: TransCanada Pipelines Limited, Spectra Energy, Natural Science and Engineering Council of Canada, Alberta Research Council

- Schedule - tasks completed during this reporting period as related to agreement with any modifications. If Completion Date is different from Scheduled Completion Date, explain.

Please see the above table for schedules. There was no any deviation from the schedules as originally planned.

- Payable Milestones - provide information sufficient for the Technical Manager to verify what percentage of work each milestone of each activity/Deliverable has been accomplished.

All the tasks defined in this quarter are performed according to schedules.

- Results and Conclusions: (Including findings, discoveries and attachments of any test data and/or pictures)

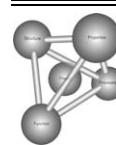
See attached files.

- Issues, Problems or Challenges: (Including anything that may cause a schedule delay)

No issues and problems for this quarter.

- Plans for Future Activity: (Including potential meetings, tests, and/or demonstrations scheduled over the next quarter.)

- To continue investigating the effect of operation conditions on crack growth



Transgranular crack growth in the pipeline steels exposed to near-neutral pH soil aqueous solutions: The role of hydrogen

W. Chen^{a,*}, Richard Kania^b, Robert Worthingham^b, Gregory Van Boven^c

^a Department of Chemical and Materials Engineering, University of Alberta, Edmonton, Canada T6G 2G6

^b TransCanada Pipelines Limited, Calgary, Canada T2P 5H1

^c Spectra Energy Transmission Limited, Vancouver, Canada V6E 3R5

Received 31 May 2009; received in revised form 17 August 2009; accepted 21 August 2009

Abstract

The aim of this investigation was to understand why some transgranular cracks developed in the pipeline steels exposed to near-neutral pH environments, typically 5% of total crack population, can propagate repeatedly and cause pipeline rupture. Crack growth in the current condition is related to two competitive processes at the crack tip: the intrinsic blunting and the extrinsic sharpening. Balance of both determines whether cracks will be dormant or actively grow. For a given pipeline, the presence of near-neutral pH environments and high residual stresses on the pipe surface determines whether a crack colony can develop, while the presence of high concentration of diffusible hydrogen is thought to determine whether repeated crack growth can occur. This is believed to be a key reason why a small fraction of cracks, typically 5% of total population, can grow repeatedly and cause pipeline rupture.

© 2009 Acta Materialia Inc. Published by Elsevier Ltd. All rights reserved.

Keywords: Steels; Corrosion; Hydrogen embrittlement

1. Introduction

It is well established that transgranular stress corrosion cracking (SCC) requires film formation on the crack walls and corrosion at the crack tip to occur simultaneously. This scenario can usually be achieved when a susceptible material is exposed to a transition zone in the polarization curve that demarcates active dissolution and passivating [1]. The above cracking prerequisite, however, is not necessary for intergranular SCC, which can occur over a wider range of potentials because chemical inhomogeneities at the grain boundary produce a different electrochemical response relative to grain material [2].

When transgranular cracking is observed in a corrosion environment that strongly passivates the materials being exposed, film rupture by localized plastic deformation from a static stress (condition of stress corrosion cracking)

becomes insignificant and crack growth would be too slow to cause any engineering concerns. Under these circumstances, cyclic loading becomes important, and can enhance the process of film rupture to make the crack grow at a rate that is of engineering significance [3,4], i.e. corrosion fatigue occurs [4].

In an environment that does not produce passivation on the material being exposed, transgranular cracking under constant stress (i.e. the condition for SCC) would be less likely to occur as corrosion will occur at the crack tip and on the crack walls as well. This could gradually turn a crack characteristic of a sharp tip into a pit (blunting) if the crack could be formed initially, for example, by a different mechanism. As a result, transgranular cracking in an environment that does not passivate the material being exposed can occur only if there exists a mechanism that could maintain the crack tip at a sharp state (e.g. at high growth rates at which crack tip blunting is negligible), or could constantly sharpen the crack tip to counterpart the blunting.

* Corresponding author. Tel.: +1 780 492 7706; fax: +1 780 492 2881.
E-mail address: Weixing.Chen@ualberta.ca (W. Chen).

Near-neutral pH groundwater that has been found to be responsible for the rupture of buried pipeline steels is an environment that causes pipeline steels to crack transgranularly, and corrodes pipeline steels without passivating them [5–9]. Fig. 1 shows the cross-section of a typical near-neutral pH transgranular crack in a pipeline steel that developed in the field. It has been found from statistical analysis of thousands of crack colonies that 95% of the crack population has a blunt tip as shown in Fig. 1 [10,11]. Cracks with such a crack tip morphology are considered to be dormant. However, the remaining 5% of the total crack population can grow continuously or repeatedly, leading to pipeline rupture. This investigation is aimed to provide some insights on the mechanisms that govern the growth of those growing cracks that take up of about 5% of the total crack population.

2. Basic considerations

To determine the prerequisite condition for these growing cracks, 5% of the total population, it might be useful to outline some key characteristics of the other 95% that remain dormant. Crack dormancy in the field occurs primarily in the stage of crack initiation and early short/shallow crack growth. The cracks formed can be better characterized as shallow notches, instead of cracks, for which fracture mechanics principles, such as stress intensity factor, cannot be applied for analysis. These defects are usually less than 1 mm deep and have very small depth/length aspect ratios, around 0.1–0.2.

Details of the initiation of the shallow cracks and early crack propagation are not the subject of this investigation. However, a brief summary is made here for the purpose of better understanding the growth behavior of cracks beyond the dormant stage that is the focus of this paper. It is generally believed that crack initiation can be caused by many different mechanisms [12–26], including preferential disso-

lution at physical and metallurgical discontinuities such as scratches [12], inclusions [13], grain boundaries, pearlitic colonies and banded structures [14–16] in the steel; corrosion along persistent slip bands induced by cyclic loading prior to corrosion exposure [14,17]; crack initiation at stress raisers such as corrosion pits [18,19]; and localized corrosion through millscale-steel galvanic effects [20]. The initiation of microstructurally short cracks, usually less than 100 μm , can occur under a constant stress loading. The early crack growth is generally believed due to the presence of high tensile residual stresses at the pipe subsurface [11,21,22], which adds to the applied stress. However, these cracks generally remain dormant for reasons yet to be determined.

Pipeline ruptures in environments that can develop the above features are usually caused by the propagation of sharp cracks (those 5% of the crack population). Therefore, special conditions must exist at some locations on the pipe surface or during certain periods of service that either make the defects maintain a relatively sharp tip or resharpen the tip after blunting. Such competitive conditions are briefly considered below based on the nature of synergistic interactions between neutral pH soil environments and the mechanical loading encountered by pipeline steels.

2.1. Under constant stress loading—scenario of stress corrosion cracking

Pipeline cracking in near-neutral pH groundwater was initially classified as SCC [5–7], implying that the crack can initiate and grow under a static load/stress. This classification was probably chosen because steel pipelines, particularly those for high-pressure gas transmission, are operated under a near-static loading condition, and furthermore high-pH SCC in steel pipelines can be reproduced in the laboratory under static loading [27–29]. However, crack growth in pipeline steels exposed to near-neutral pH environment has never been observed under static loading. This observation, however, does not exclude the possibility that crack initiation as outlined previously results in the formation of short cracks mostly at a dormant state through various processes in which fracture mechanics principles are not applicable [14,15,23,24]. Nevertheless, a pre-existing axial crack would become dormant under static loading in near-neutral pH environments. In fact, mild mechanical cycling in near-neutral pH environments would also lead to crack dormancy as is demonstrated in Ref. [30]. This coincides with the fact that 95% of the crack population are in a dormant state once they reach ~ 0.5 mm in depth [10,11].

Fig. 2 shows various competitive factors both for crack sharpening as a prerequisite to active crack growth and for blunting leading to crack dormancy. A predominant factor in near-neutral pH soil environments that causes crack tips to blunt is the general corrosion occurring at the crack tip and on crack walls since these environments do not cause pipeline steels to passivate [8]. The second factor that can

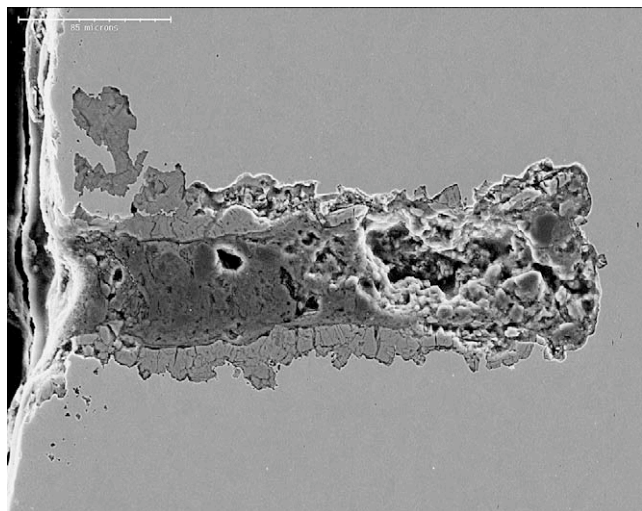


Fig. 1. Typical morphology of a dormant crack found in buried pipeline steel exposed to near-neutral pH soil water solution in the field.

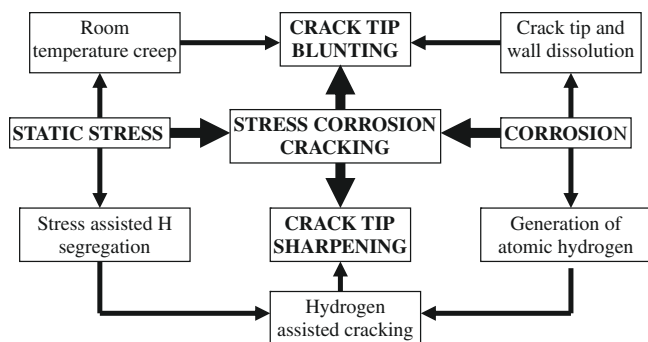


Fig. 2. A schematic showing the competition between crack tip blunting and crack tip sharpening in the pipeline steels exposed to near-neutral pH environments under constant stresses (conductive to SCC).

contribute to the crack tip blunting is room temperature creep (RTC), which is unique to pipeline steels and can be very high depending on the type of pipeline steel and prior loading history of the steel [31–34]. Room temperature creep will occur at the tip of crack when the crack tip is stressed.

Opposite to the process of blunting, segregation of atomic hydrogen to the hydrostatic zone and the highly deformed areas ahead of the crack tip may be the main reason for crack sharpening [35]. Under the circumstances, hydrogen-induced microcracks (HICs) may be initiated by the combined effect of high hydrostatic stresses in the plastic zone, increased hydrogen segregation and the weakest link sites, such as grain boundaries and inclusions, in the plastic zone ahead of the crack tip. The microcracks that form in the plastic zone link up with the main crack, resulting in crack extension [36,37] and resharpening of the blunt tip. On the other hand, hydrogen adsorption-induced cleavage (also called stress-sorption cracking), originally proposed by Uhlig, may also take place and result in direct sharpening of the blunt tip [38].

The above sharpening process is unlikely to occur under static loading as cracks are mostly dormant, and at least when cracks are around 1.0 mm deep. Proof of the above competition is the observation of sharp microcracks in the plastic zone ahead of the tip of a dormant crack/notch about 0.8 mm deep [9]. However, the microcracks did not link up with the main crack, indicating that initiation of such microcracks is possible, but its propagation to the root of the main crack to resharpen it has not occurred. Further explanation on this observation is provided in Section 4.1.

2.2. Under cyclic stress loading—scenario of corrosion fatigue

When cyclic loading is present in the loading scheme, the blunting mechanisms as discussed previously in the SCC type of loading scenario are still applicable, except for an attenuation of low-temperature creep-related blunting process as low-temperature creep increases with an increase in

the applied stress and creep time. Therefore, this type of blunting would be more profound at lower loading frequencies and slower crack growth rates, both of which allow more time for creep to proceed at the crack tip. An analysis of competitive processes for crack tip blunting and sharpening in the case of cyclic loading is shown in Fig. 3.

Recently, we have analyzed crack growth data both from laboratory tests using compact tension (CT) specimens and from full-scale tests of shallow cracks [30,39]. It has been found that the crack growth rate per cycle (da/dN) can be correlated by $\Delta K^2 K_{\max}/f^\alpha$, where ΔK is the stress intensity factor range, K_{\max} is the maximum stress intensity factor, f is the loading frequency and α is a factor related to corrosivity of soil environments. This correlation enables the determination of threshold $\Delta K^2 K_{\max}/f^{0.1}$ values for long cracks such as in a test using a CT specimen. The above growth correlation appears also true for small/shallow cracks in full-scale tests except that small/shallow cracks were found to grow at appreciable rates below the threshold of long cracks [39], a well-understood phenomenon in fatigue [40,41].

The fact that crack growth is possible under cyclic loading but not under SCC loading implies the effectiveness of crack sharpening by fatigue in near-neutral pH soil environments, a well-understood phenomenon in the field of fatigue. However, 95% of the cracks in the field remained dormant, suggesting that sharpening and/or resharpening of crack by the type of fatigue loading encountered in the field is not predominant, or at least is not the only factor, as the dormant cracks, representing 95% of total crack population, are subjected to the same loading schemes as those 5% of cracks that do grow.

Hydrogen-related sharpening should also exist under fatigue loading. However, this sharpening mechanism should be most influential under SCC loading in terms of

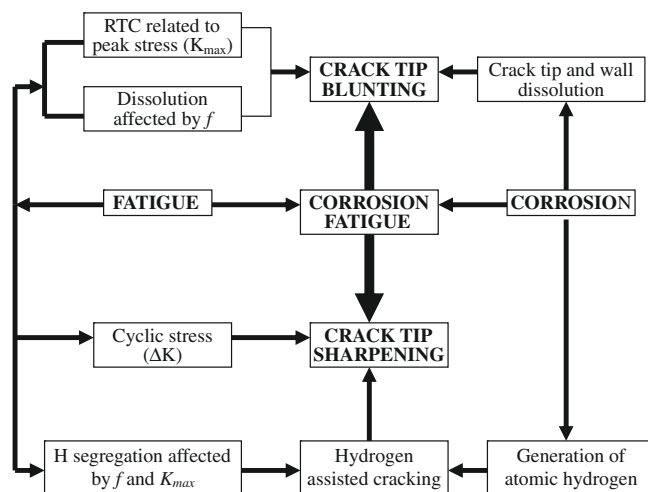


Fig. 3. A schematic showing the competition between crack tip blunting and crack tip sharpening in the pipeline steels exposed to near-neutral pH environments under cyclic loading conditions (conductive to corrosion fatigue).

hydrogen segregation in comparison with fatigue loading. However, crack growth does not occur under SCC loading, indicating that hydrogen-related sharpening cannot act alone to resharpen the crack as discussed previously.

As a result, the mechanism(s) governing crack resharpening in the field cannot be either purely fatigue- or hydrogen-related. Instead, a synergistic interaction of both is most likely the case. The former factor is common to all the cracks in the system; the latter would be very location dependent and could interact with the former factor to make some of the cracks, typically 5% of the total population, grow continuously or repeatedly. This investigation is aimed primarily to determine the location-specific conditions involving synergistic interactions of realistic fatigue loading (characteristic of high stress ratio and very low loading frequency [42]) and hydrogen-assisted crack tip sharpening and resharpening in pipeline steels exposed to typical near-neutral pH soil environments.

It should be noted that the above considerations are only limited to two of the three essential factors on corrosion cracking, i.e. stress and environment. The third factor, material, is important when discussing the susceptibility of different materials or microstructures. For a given pipeline steel, the fabrication conditions can be considered to be similar. Variation in microstructural features are usually at the micrometer level (e.g. inclusions and grain boundaries), which may affect the growth for a short period, such as via crack initiation, except for the effect of residual stresses and banded microstructures. The effect of residual stress is also very location specific and may play a decisive role in the process of continuous or repeated growth of those 5% of total cracks responsible for pipeline rupture. This factor of residual stresses has been considered in detail in previous research [11,21–22], and will be discussed as it is needed when stress and environmental factors are considered. The banded microstructures are normally seen in the central region of the pipe wall, and the bands are oriented along the pipeline length direction. The effect of these microstructures on crack growth in the pipe thickness direction, particularly in the early and intermediate stage of crack growth, would be limited.

Table 1
Chemistry of synthetic solutions used in the investigation.

Chemicals	C2	NOVATW
MgSO ₄	0.0274	
CaCl ₂	0.0255	
CaCO ₃	0.0606	0.23
NaHCO ₃	0.0195	0.437
KCl	0.0035	0.015
CaSO ₄ 2H ₂ O		0.035
pH (5% CO ₂ , N ₂ balance)	6.29	7.11

3. Experimental

An X-65 pipeline steel was used in this study; its chemical composition (wt.%) is listed in Table 2. The X-65 pipeline steel was characterized to be susceptible to near-neutral pH SCC [14,15,43]. CT specimens were machined from the X-65 pipe with the machined notch perpendicular to pipe circumferential direction. Each of the specimens was polished to produce a scratch-free surface prior to mechanical

Table 2
Chemical composition (wt.%) of the X-65 pipeline steel used in this investigation.

Elements	Composition, wt.%
C	0.12
Mn	1.5
P	0.017
S	0.0046
Si	0.26
Cu	0.014
Ni	<0.02
Cr	0.065
Mo	<0.03
V	<0.01
Nb	0.049
Ti	<0.005
Al	0.029
Sn	0.0016
Ca	0.0012
B	<0.0005
Pb	<0.01
Zr	<0.002
Co	0.004

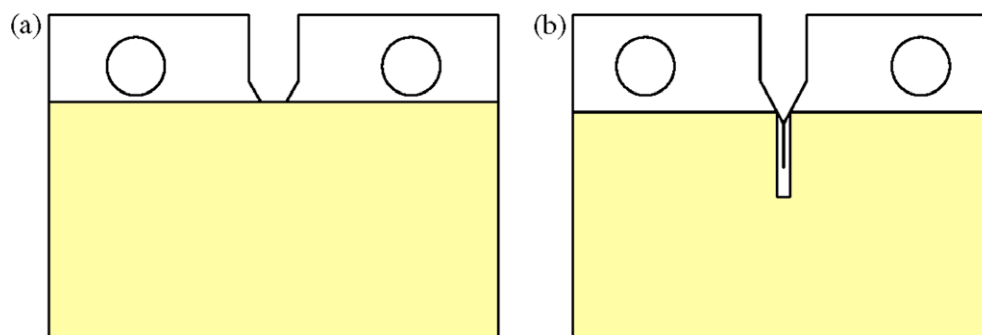


Fig. 4. Schematic illustration showing coatings (shaded area) applied to the surface of CT specimens: (a) complete coverage; (b) partial coverage.

loading. The thickness of the specimen was around 9.0 ± 0.2 mm.

The machined CT specimen was pre-fatigue cracked for the initiation of a sharp crack tip from the machined notch, which was performed according to ASTM E647-93. The pre-fatigued crack length on both sides of the surface was controlled to be 2–3 mm long. The difference in crack length on both sides of the surfaces of each specimen was less than 0.2 mm. After pre-fatigue cracking, the specimen was cyclically loaded in near-neutral pH synthetic soil solutions. A triangle waveform was used with a loading frequency in the range of 0.005–0.0025 Hz, and a stress R -ratio of 0.6 and 0.7. The maximum and minimum stress was controlled to achieve a maximum stress intensity factor (K_{\max}) in the range of 35–55 $\text{MPa}\sqrt{\text{m}}$, and the stress intensity factor range (ΔK) from 10 to 28 $\text{MPa}\sqrt{\text{m}}$. The testing was performed on a pneumatic cyclic loading frame horizontally laid on the benchtop; the CT specimen was pin-hole loaded and sealed in the test cell with the test solution filled up to the middle of the machined notch.

CT specimens in some tests were coated with epoxy to prevent direct contact of soil solutions. As shown in Fig. 4, the coating was applied either to cover the entire surface (Fig. 4a), or all the surface areas except for a narrow region containing the crack. In both the cases, test solution was added to a position above the coated line.

Two types of synthetic soil solutions were used in this investigation: the NOVA Trapped Water (NOVATW) and C2 solution [44]. Their chemical compositions are listed in Table 1. All the solutions were purged with 5% CO_2 , N_2 balance to achieve a near-neutral pH value. The test solution was contained in a sealed glass cell after being purged by 5% CO_2 , N_2 balance for at least 24 h. Gas purging was also maintained during corrosion exposure.

Crack growth was monitored by a self-assembled potential drop system. Details of this testing system were reported in Ref. [30]. The measured potential was converted to actual crack length by measuring the crack length on the fractured specimen. For the current system, the conversion factor was found to be 25.5 ± 3.5 mm mV^{-1} , based on a number of tests with small amounts of total crack propagation.

After corrosion exposure, the test specimen was cleaned and sectioned for scanning electron microscopy (SEM) examination.

4. Results and discussion

4.1. Competition between crack tip blunting and crack tip sharpening under static stress

Since a near-neutral pH environment does not cause pipeline steel to passivate, active dissolution would produce crack tip bluntness if it is initially sharp. Therefore, alternative processes must be present concurrently or sequentially to keep the crack tip sharp or to resharpen the blunt crack tip in order to produce active growth. Such a dilemma can be best seen from the comparative tests shown in Fig. 5. In Fig. 5, two CT specimens exposed to NOVATW and C2 solutions, respectively, were subjected to the same mechanical loading schemes. The tests started at $\Delta K = 12$ $\text{MPa}\sqrt{\text{m}}$ and $K_{\max} = 35.3$ $\text{MPa}\sqrt{\text{m}}$ for about 175 h. This was followed by a hold at 35.3 $\text{MPa}\sqrt{\text{m}}$ for a period of about 10 days. No crack growth was observed during the hold for both specimens. However, when the same cyclic loading condition was resumed, crack growth started immediately in the specimen exposed to C2 solution, but the dormant state remained in the specimen exposed to NOVATW. At

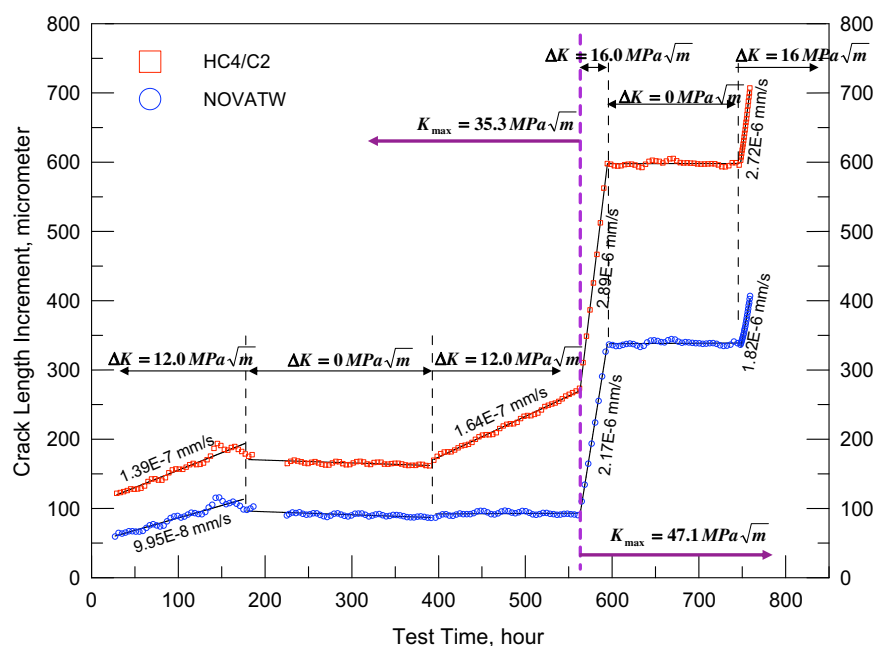


Fig. 5. Crack length increment as a function of test time in two different soil solutions.

higher K_{\max} and ΔK loading, however, no dormancy in NOVATW was observed when cyclic loading was restarted. During all the holds, no crack growth was detected, indicating the absence of SCC, further confirming the suggestions made in Section 2.

Fig. 6 shows the cross-sectional morphology of the crack at the location of static holds when exposed to NOVATW. Blunting was evident at the crack tip of both the holds at $K_{\max} = 35.3 \text{ MPa}\sqrt{\text{m}}$ for 10 days and $K_{\max} = 47.1 \text{ MPa}\sqrt{\text{m}}$ for about 7 days, respectively. It was determined from weight loss experiments that the corrosion rate of pipeline steel in C2 solution was about 3 times higher than that in NOVATW [30]. Due to low dissolution rate in NOVATW [30], blunting was probably caused by plastic deformation, as the crack tip is broadened in a 45° direction (see arrows in the insert) where the shear stresses for plastic deformation are the highest. Similar features were also observed when the hold was conducted at $K_{\max} \approx 35.3 \text{ MPa}\sqrt{\text{m}}$. In both cases, plastic

deformation appears to be produced by low-temperature creep [31–34].

In contrast, there was massive corrosion at the crack tip during the hold in C2, as shown in Fig. 7, which appears blunter than that seen in NOVATW. Evidence of plastic deformation-induced blunting was not clearly observed in C2 solution, probably due to increased dissolution in the solution that destroyed the 45° shear paths observed at the crack tip exposed to NOVATW. A stress intensity factor of about $35 \text{ MPa}\sqrt{\text{m}}$ can be achieved when a semi-elliptical crack of about 10–20% of wall thickness in depth and about 10 times of depth in length direction in a X-65 pipeline steel is loaded to about 75% SMYS (specified minimum yield strength). A stress intensity factor of $47.1 \text{ MPa}\sqrt{\text{m}}$ can be achieved at the crack tip during hydrostatic testing used for detecting critical sizes of cracks in pipelines [45].

Although crack growth under cyclic loading is also presented in Fig. 5, here we just focus on crack growth behavior under static loading. The fact that a crack does not grow under constant K_{\max} simply suggests that crack tip blunting prevails over crack tip sharpening. The blunting can be achieved by low-temperature creep at the crack tip alone, while corrosion further intensifies the bluntness. A key indicator for the occurrence of sharpening would be the detection of crack growth either by corrosion at the crack tip in the growth direction or by HICs in the plastic zone ahead of the crack tip. It was also suggested that hydrogen-facilitated corrosion may contribute to the growth of crack [46]. Since no crack growth was detected during the static hold, hydrogen-facilitated corrosion may have occurred, but should not be a concern as it did not

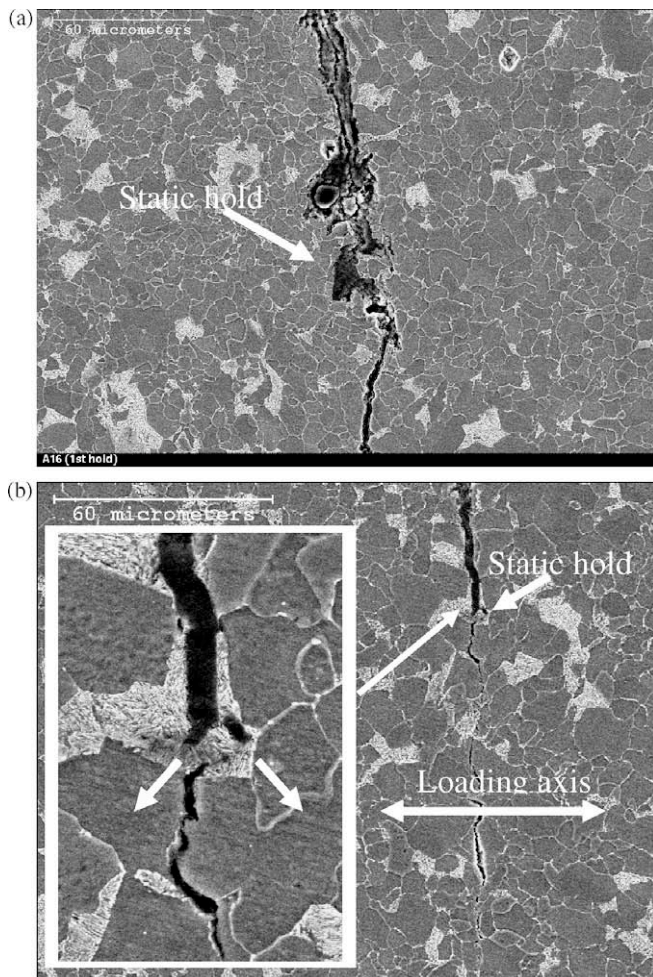


Fig. 6. Crack tip morphology of CT specimen after static holds at two constant stress intensity factors in NOVATW solution: (a) hold at about $35.3 \text{ MPa}\sqrt{\text{m}}$ for 10 days; (b) hold at about $47.1 \text{ MPa}\sqrt{\text{m}}$ for 7 days. The insert in (b) is a magnified view of the crack tip at the position of static hold.

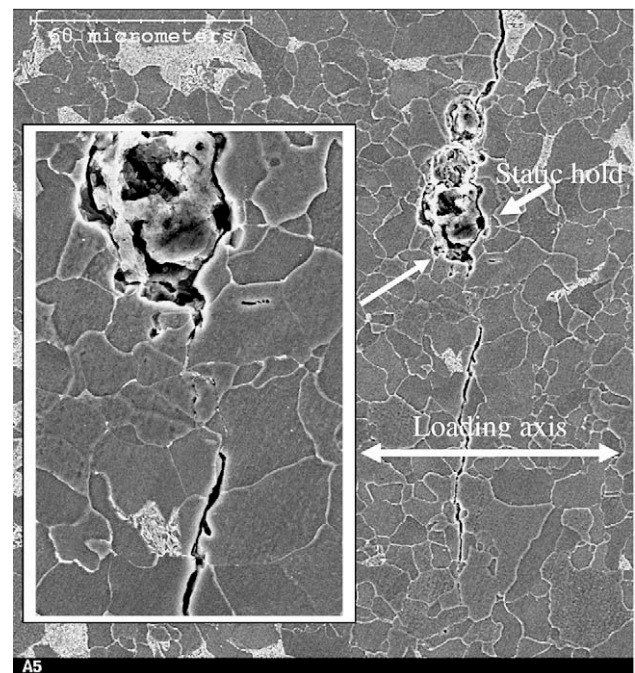


Fig. 7. Crack tip morphology of CT specimen after a static hold at about $47.1 \text{ MPa}\sqrt{\text{m}}$ for 7 days in C2 solution. The insert is a magnified view of the crack tip at the position of static hold.

yield any crack growth, i.e. there was corrosion, but no corrosion-induced cracking. This seems consistent with recent thermodynamic analysis that SCC of pipeline steel in anaerobic groundwater of near-neutral pH is unlikely to be related to the hydrogen-facilitated anodic dissolution mechanism [47].

There are a number of fundamental reasons why crack growth through the initiation of HICs in the plastic zone ahead of the crack tip is unlikely to occur under the static loading in the current system. First, near-neutral pH solutions, unlike the acidic environments found in oilfields, produce very limited hydrogen generation. Experimental investigation has shown that the concentration of diffusible hydrogen even under adequate cathodic protection is less than 1/10th of the critical diffusible hydrogen concentration required to induce hydrogen blistering (formation of microcracks near the subsurface) in pipeline steels [48,49]. Considering possible segregation of diffusible hydrogen to the crack tip [35], it might be possible to initiate microcracks at the weakest links, such as inclusions, grain boundaries and pearlite/ferrite interfaces located in the plastic zone, which are also strong traps of diffusible hydrogen. However, additional conditions must be met in order to propagate these microcracks. Such prerequisites have been determined in detail for the case of cleavage fracture in low-carbon steels under impact loading [50]. Although various mechanisms are available, the main limiting factors are the size of the microcracks formed and the range of high hydrostatic stress present in the plastic zone. A microcrack after initiation can propagate continuously only when it reaches a critical size (governed by fracture mechanics). Otherwise, it will be arrested, unless there is a sudden increase in mechanical driving force. The fact that no crack growth can be observed under static loading suggests that microcracks might be either less likely to be initiated due to extremely low diffusible hydrogen at most locations or impossible to propagate after initiation, probably due to their small dimensions.

4.2. Competition between crack tip blunting and crack tip sharpening under cyclic loading

Crack growth started immediately after cyclic loading was executed following static loading in C2 solution in both cyclic schemes. In contrast, cracks remained dormant during cyclic loading after static hold at $K_{\max} \approx 35.3 \text{ MPa}\sqrt{\text{m}}$ in NOVATW solution. At higher K_{\max} , crack growth was detected immediately after the static hold, which produced crack tip blunting.

Since the static hold (SCC loading) has caused crack tip blunting in both solutions, the reactivation of a dormant crack by fatigue loading indicates the sharpening effect of cyclic stresses, which is well understood in the field of fatigue.

Although the crack tip exposed to C2 solution was blunter due to its higher corrosion rate, it was surprising that at low K_{\max} and ΔK loading condition, crack growth was

reinitiated in the specimen exposed to C2; this is unexpected because of the blunter crack tip. Since the external mechanical driving force for crack growth was controlled to be the same, there must be other factors that can act together with the cyclic sharpening process to resharpen the crack tip.

It is often suspected that hydrogen may play a key role in crack growth in near-neutral pH environments. The source of hydrogen in the current system is primarily related to the dissolution of Fe, which generates electrons, which are used for the reduction of hydrogen ions in the system. Because of the higher dissolution rate, more hydrogen atoms should be generated in C2 solution than in NOVATW.

Based on the above analysis, it is believed that the different response to cyclic loading after the static hold at $K_{\max} = 35.3 \text{ MPa}\sqrt{\text{m}}$ between C2 and NOVATW solutions is caused by hydrogen effects. Although the higher rate of dissolution in C2 solution yielded a blunter crack tip, it generates more hydrogen and hence assisted crack resharpening to a greater extent.

Dislocation slip is usually involved in the microprocessing of crack growth under cyclic loading. It has been well documented that hydrogen enhances dislocation mobility along slip bands and results in slip localization; these slip bands in turn accelerate the trapping and diffusion of hydrogen [51–53]. This mechanism of hydrogen–slip band interaction enhances crack growth under cyclic loading [51,53]. Specially designed crack growth tests were performed and are presented in the next section to further elucidate the mutual interaction between hydrogen and cyclic loading in crack growth in pipeline steels exposed to near-neutral pH environments.

4.3. Role of hydrogen

In the current test setup, hydrogen could be generated at any surfaces that were exposed to the aqueous solution. However, only the hydrogen atoms that are diffused and segregated to the hydrostatic zone or to areas with the highest strain accumulation ahead of the crack tip have an effect on crack growth. When a positive hydrostatic stress exists, hydrogen diffuses to this region in order to lower the chemical potential. Conversely, hydrogen will move out of areas that experience compressive hydrostatic stress. The equilibrium concentration of hydrogen in a stressed lattice, C_L^σ , is [35]:

$$\frac{C_L^\sigma}{C_L^0} = \exp\left(\frac{\sigma_h \bar{V}_H}{3RT}\right) \quad (1)$$

where C_L^0 is the lattice concentration of hydrogen in the absence of stress, C_L^σ is the steady-state lattice concentration of hydrogen under hydrostatic stress, \bar{V}_H is the partial molar volume of hydrogen, σ_h is the hydrostatic stress, R is the universal gas constant ($8.314 \text{ J mol}^{-1} \text{ K}^{-1}$) and T is the absolute temperature of the system.

Although corrosion at the crack tip produces hydrogen that can diffuse a short distance from the crack tip, the segregation is related to the nominal lattice hydrogen concentration, as given in Eq. (1). A supply of hydrogen resulting only from corrosion at the crack tip in the current situation would yield limited lattice hydrogen as hydrogen atoms would diffuse down a concentration gradient to any regions with lower hydrogen concentration. The surface of the CT specimen is believed to be a main source of lattice hydrogen, as a result of general corrosion; this hydrogen diffuses toward the center of the CT specimen and reaches an equilibrium over a certain length of time depending on the diffusivity of hydrogen, the test temperature and the thickness of the specimen.

Comparative tests were performed to determine the effect of hydrogen on crack growth in near-neutral pH environments. Each set of comparative tests consisted of specimens that differed with respect to their surface conditions: one had bare surfaces; the remaining two were

coated with epoxy as shown in Fig. 4a and b, respectively. Three tests were performed in the same environment with identical starting loading conditions: $K_{\max} = 35.3 \text{ MPa}\sqrt{\text{m}}$, $\Delta K = 12.0 \text{ MPa}\sqrt{\text{m}}$ and $f = 0.005$. These loading conditions yielded a value of $(\Delta K^2 K_{\max} / f^{0.1} = 8610 \text{ MPa}^3 \text{ Hz}^{-0.1})$, which is slightly above the threshold of C2 solution ($\sim 8500 \text{ MPa}^3 \text{ Hz}^{-0.1}$), but slightly below that of NOVATW solution ($\sim 9000 \text{ MPa}^3 \text{ Hz}^{-0.1}$) [30].

As shown in Fig. 8a, the three tests in NOVATW went to a dormant state at a testing time of about 400 h, which is consistent with the fact that the loading condition was below the threshold. In C2 solution, however, crack growth was evident (Fig. 8b), but varied significantly depending on the surface condition. Fig. 9 shows the growth rate (da/dN) as a function of testing time for all three tests in C2 solution. For the uncoated CT specimen, a three-stage process can be seen: an initial stage of about 275 h during which the growth rate was nearly insensitive to the testing time; a second stage with a rapid increase in growth rate; and a third stage during which there was a reduced growth rate dependence of testing time. For the CT specimens with epoxy-coated surfaces, the initial stage was similar to that found with the uncoated CT specimen except for a slightly lower growth rate; a decrease in growth rate was seen following the initial stage; and an increase in growth rate occurred at about 500 h. The partially coated specimen as shown in Fig. 4b seems to exhibit a growth behavior similar to the completely coated specimen except for a slightly higher overall growth rate.

Similar tests were also conducted at a loading condition with much higher $\Delta K^2 K_{\max} / f^{0.1}$ value. Fig. 10 shows the change in growth rate with testing time for specimens with uncoated surfaces in two different solutions. The tests at

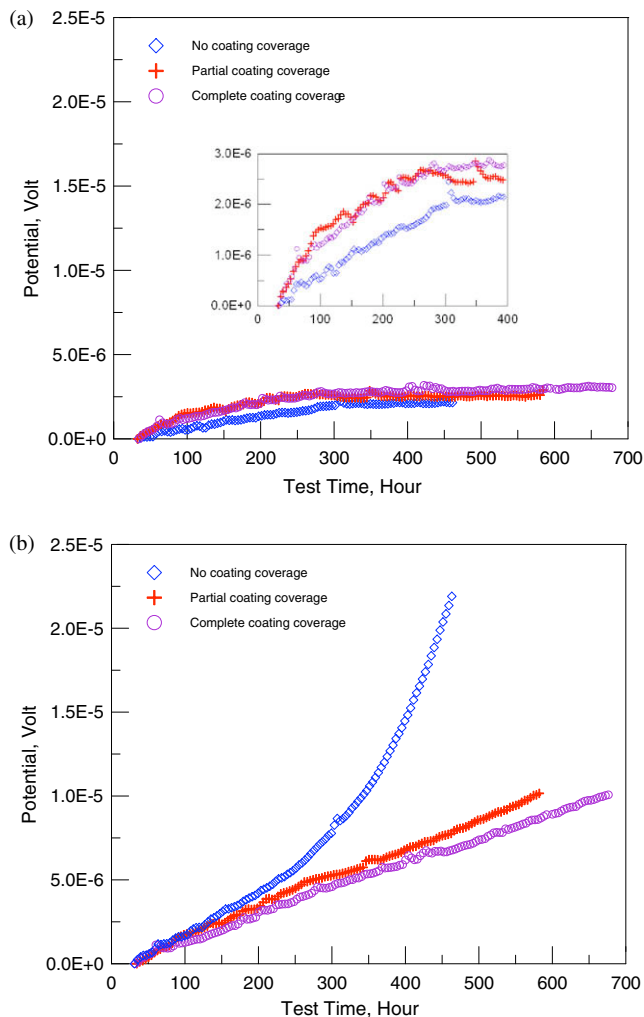


Fig. 8. Change in measured potential as a function of test time for three specimens tested in NOVATW (a) and C2 (b) solutions. All the tests were conducted with the same starting conditions at $K_{\max} = 35.3 \text{ MPa}\sqrt{\text{m}}$, $\Delta K = 12.0 \text{ MPa}\sqrt{\text{m}}$ and $f = 0.005 \text{ Hz}$.

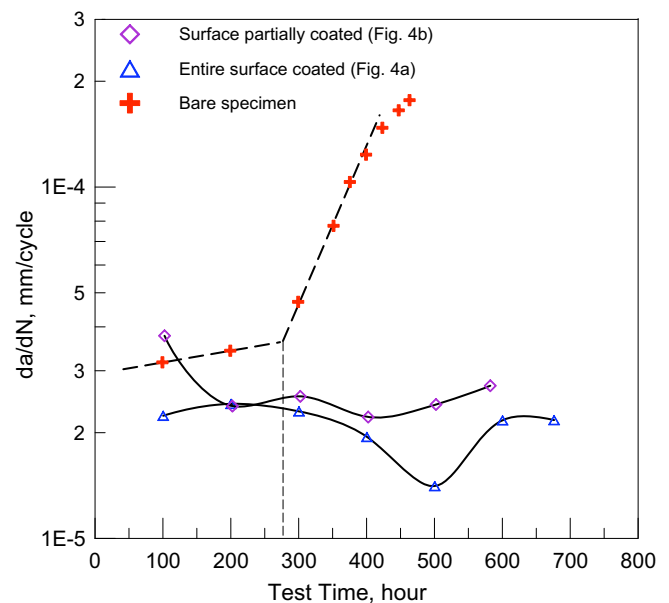


Fig. 9. Crack growth rate as a function of test time for three specimens tested in C2. All the tests were performed at the same starting conditions at $K_{\max} = 35.3 \text{ MPa}\sqrt{\text{m}}$, $\Delta K = 12.0 \text{ MPa}\sqrt{\text{m}}$ and $f = 0.005 \text{ Hz}$.

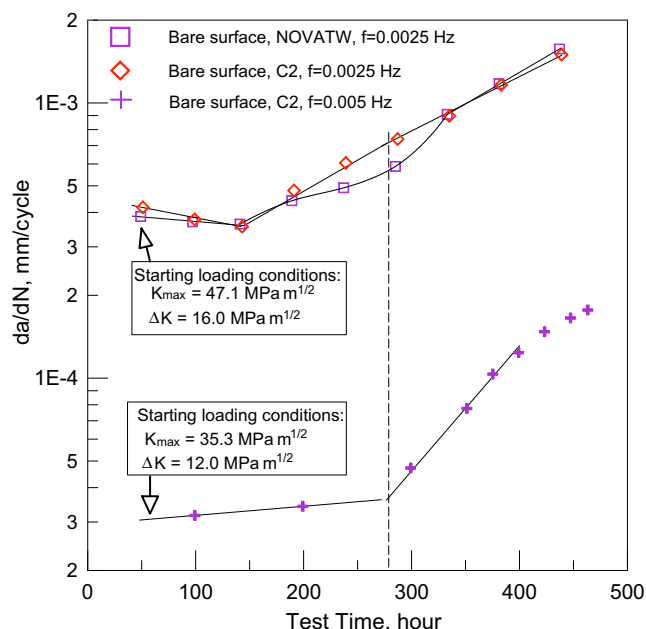


Fig. 10. Crack growth rate as a function of test time.

high loading conditions seemed to exhibit different growth rate stages. The growth rate was seen to decrease with testing time in the initial stage. This is followed by a continuous increase in growth rate. The transition occurring at around 275 h seen at low loading conditions was not very obvious for some of the high $\Delta K^2 K_{\max}/f^{0.1}$ tests.

The above inconsistency can be understood when the effect of hydrogen is considered. As indicated previously, it is necessary to generate hydrogen on the surface of the CT specimen in order to reach an equilibrium lattice hydrogen concentration in the specimen so that a high hydrogen concentration can be established in the plastic zone affecting crack growth. To reach equilibrium, a critical time of diffusion must be available. The diffusivity of hydrogen in the steel was determined to be about $2 \times 10^{-7} \text{ cm}^2 \text{ s}^{-1}$ [54]. For a test duration of 275 h, this would yield a diffusion distance of $\sqrt{Dt} = \sqrt{2 \times 10^{-7} (\text{cm}^2/\text{s}) \times 275 (\text{hr}) \times 3600 (\text{s})} = 4.45 \text{ mm}$, which is about a half of the thickness of CT specimen used in the current investigation ($\sim 4.5 \text{ mm}$). This 275 h test duration represents the minimum time required for hydrogen to reach through the entire specimen thickness, although the peak equilibrium flux would take longer to establish. Therefore, it is reasonable to conclude that the rapid increase in crack growth rate for the uncoated specimen corresponds to the onset of the hydrogen effect on crack growth. When CT specimens were coated, hydrogen was generated only by corrosion at the crack tip, which is very limited in terms of its effect on crack growth. This limited influence does not yield a significant change in growth rate with increasing time and stress intensity factor.

The above critical time of hydrogen effect is not very obvious in the growth curve obtained at high $\Delta K^2 K_{\max}/f^{0.1}$ loading. It is believed that this is caused by

the high growth rate due to more aggressive cyclic loading conditions. The total crack growth in the low ($\Delta K^2 K_{\max}/f^{0.1}$) test (bare specimen in Fig. 5) was about 0.5 mm, which has caused a change in K_{\max} and ΔK of 1.3 and 0.44 MPa $\sqrt{\text{m}}$, respectively, for the entire test. In the transition region around 275 h, the growth rate was very low, and K_{\max} and ΔK can be assumed to be constant (Fig. 5b). The change in growth rate is therefore a true reflection of environmental (hydrogen) effects on crack growth. On the other hand, the growth rate in the test with high ($\Delta K^2 K_{\max}/f^{0.1}$) value represents the combined effect of environment and mechanical driving force ($\Delta K^2 K_{\max}$). As a result, the distinct effect of environment is attenuated in the growth rate curve.

When the growth data at the loading condition with high ($\Delta K^2 K_{\max}/f^{0.1}$) value was normalized by ($\Delta K^2 K_{\max}/f^{0.1}$) [30], the transitional effect of hydrogen becomes more clear, as shown in Fig. 11. The curve showed an inflection at around 275 h, consistent with the time determined from the tests conducted at a ($\Delta K^2 K_{\max}/f^{0.1}$) value near the threshold.

The above hypothesis is also consistent with the growth behavior of coated specimen loaded at high ($\Delta K^2 K_{\max}/f^{0.1}$) values, as shown in Fig. 12, where the growth rate in the two test solutions is presented. The growth rate of coated specimens did not show an inflection, suggesting that the transitional behavior related to the hydrogen effect did not occur. The growth rate curves of the coated specimens are below those of the uncoated specimens, reflecting the contribution of hydrogen to crack growth, which is smaller than that observed at low $\Delta K^2 K_{\max}/f^{0.1}$ loading.

There was also a transitional behavior occurring at around 125 h, before which crack growth rate was seen

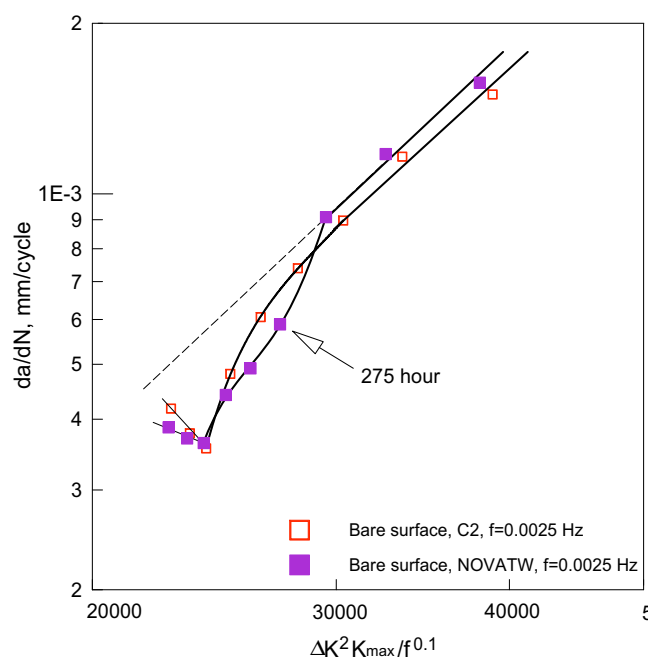


Fig. 11. Crack growth rate as a function of $\Delta K^2 K_{\max}/f^{0.1}$.

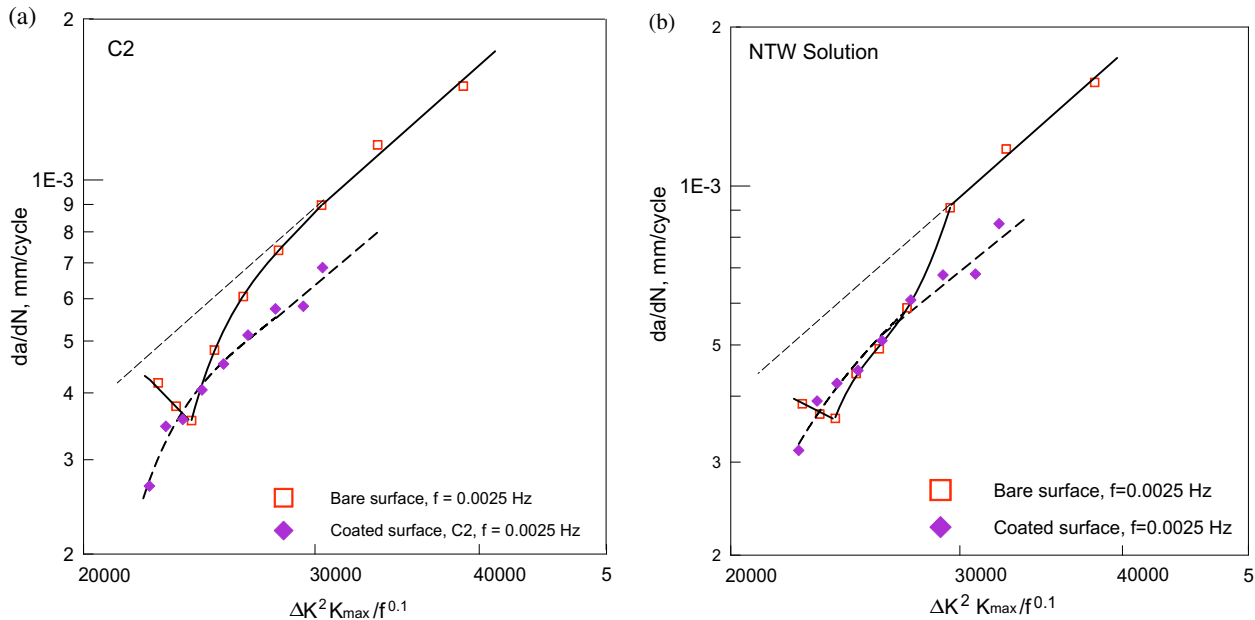


Fig. 12. Comparison of crack growth behavior between the bare CT specimen and the coated CT specimen: (a) in C2; (b) in NOVATW. All the tests were conducted with a starting $K_{\max} = 47.1.3 \text{ MPa}\sqrt{\text{m}}$, $\Delta K = 16.0 \text{ MPa}\sqrt{\text{m}}$ and $f = 0.0025 \text{ Hz}$.

to decrease with increasing time. This behavior is believed to be related to morphological changes in the crack tip caused by corrosion. As observed in Fig. 5, a hold at constant stress did not yield any crack growth but led to crack tip blunting through corrosion. Because of the non-passivating nature of the current corrosion system, corrosion at the crack tip may contribute to crack growth to some extent, but primarily produces general corrosion and leads to crack tip blunting. The latter would decrease the mechanical driving force for crack propagation.

Previous investigation has shown that the corrosion rate of near-neutral pH environments as determined by weight loss measurements was the highest at the beginning of corrosion exposure but decreases gradually to a stabilized value after about 4 days of corrosion exposure [30]. The high crack growth rate at the beginning of testing may result from the higher corrosion rate of near-neutral pH environments and a sharp crack tip from pre-fatigue cracking in air. The reduced crack growth rate reflects the fact that the corrosion rate of near-neutral pH environment is decreased and the crack tip becomes blunter due to corrosion. Crack growth rate increases as hydrogen effects become important. In this case, the hydrogen effects are produced by hydrogen atoms diffused from cracked surfaces and the crack tip. Because of the short diffusion distance, an increase in growth rate was seen well before 275 h, but the increase in growth rate was small due to the limited amount of hydrogen generated as discussed before.

When the entire surface is coated, the test solution comes in contact with the steel only through the top opening. Because the near-neutral pH condition in the current system is maintained by continuous bubbling of 5%

$\text{CO}_2 + \text{N}_2$ through a sealed testing cell, corrosion at the crack tip would be limited due to longer diffusion length of CO_2 gas and other corrosive species. The crack growth would be primarily determined by the mechanical driving force applied to the crack tip. As the crack propagates, hydrogen generated at the crack tip may diffuse to the plastic zone and make some contribution to the crack growth rate. This process lasted throughout the duration of the test. As a result, only a slightly lower growth rate was detected at the beginning of testing, reflecting the time required to achieve equilibrium between the generation of hydrogen at the crack tip and the diffusion of hydrogen to the plastic zone.

The findings above seem very consistent with the growth behavior observed from tests conducted at low ($\Delta K^2 K_{\max}/f^{0.1}$), as shown in Fig. 9. The CT specimen with coated surfaces (Fig. 4a) has a lower growth rate than that of bare specimen, due to diffusion-controlled growth phenomena as discussed before. Because of a small change in mechanical driving force, the growth rate may increase slightly when hydrogen generated at the crack tip has an effect on growth rate. However, the crack growth rate should decrease gradually with increasing time due to increased crack tip blunting. At the same time, crack growth may gradually increase the mechanical driving force, which would increase the crack growth rate due to an increase in ($\Delta K^2 K_{\max}/f^{0.1}$). The latter prevails after an extended test, resulting in an increase in crack growth rate as seen at about 500 h.

To further reveal the relative effect of hydrogen on crack growth rate at different ($\Delta K^2 K_{\max}/f^{0.1}$) loading conditions, two crack growth curves obtained in C2 solution, as shown in Fig. 10, were plotted together as a function of

$(\Delta K^2 K_{\max}/f^{0.1})$ in Fig. 13. The dashed line fits only the growth data with full hydrogen effects. The extensive test data reported in Ref. [30] were not included in Fig. 13 for reasons of simplicity. As seen in Fig. 13, the crack growth rate data obtained after hydrogen equilibrium is reached in the specimen can be fit by the same line regardless of their difference in $(\Delta K^2 K_{\max}/f^{0.1})$. Prior to the hydrogen equilibrium, the crack growth rate at high $(\Delta K^2 K_{\max}/f^{0.1})$ loading is only slightly lower than that defined by the dashed line, indicating the reduced effect of hydrogen under aggressive loading conditions. In contrast, the deviation is very large at low $(\Delta K^2 K_{\max}/f^{0.1})$, suggesting a significant contribution of hydrogen to crack growth, which in fact determines the occurrence of the threshold.

4.4. Implications for pipeline cracking in the field

4.4.1. Crack growth controlling steps

This investigation has clearly demonstrated the critical role played by hydrogen in the crack growth of pipeline steels exposed to near-neutral pH environments. Crack tip blunting can be considered to be an intrinsic nature of the crack growth in pipeline steels—a near-neutral pH system—which originates from the low-temperature creep deformation due to near-static loading (conductive to SCC) and slow loading rate (conductive to fatigue at very low frequency), and the active dissolution over the deformed crack tip without producing passivation (see Figs. 2 and 3). At the same time, extrinsic processes resulting in crack tip sharpening occur concurrently or sequentially, and are related to the process of cyclic loading and the hydrogen effects as described in the current investigation. The balance of intrinsic and extrinsic factors deter-

mines whether cracks will be dormant or grow actively. This unique balance also varies with the stage of crack development.

Step 1. Crack initiation and microstructurally short cracks. As discussed previously, the stage of crack initiation involves some galvanic process that is dependent on the microstructure and/or the surface. Fracture mechanics principles cannot be applied.

Step 2. Growth of mechanically short/shallow cracks. Mechanically short cracks are those cracks with a dimension ranging from 0.1 to 1 mm, for which fracture mechanics principles can be applied [55]. Both field characterization and laboratory testing have shown that crack growth is possible only if the pipe subsurface is under high tensile residual stresses, which adds to the external stress and makes the mechanical driving force sufficient to produce crack growth [11,21,22].

The presence of high tensile residual stress near the subsurface is a key to the formation of crack colonies. Since residual stresses are not uniformly distributed, this explains why crack colonies are very location dependent. In other words, identical environmental conditions may not cause the formation of crack colonies; individual cracks in a crack colony can be short or long depending on the range of high tensile residual stress being extended in the depth direction [11,21,22].

The above tensile residual stresses are categorized as macroscale residual stresses (Type I), which vary continuously over at least several grain diameters, and are usually caused by, for example, bending of steel plate during pipe forming, different cooling rates through the wall thickness and along the surface during rolling, localized plastic deformation during handling, etc. If high tensile residual stresses are present at the outside diameter (OD) surface, there must exist regions with compressive stresses to equilibrate this stress. It was found that the positive residual stresses extended to different depths at the OD surface, but usually below 2 mm [21]. These high tensile residual stresses are necessary for the formation of crack colonies; however, they are not the necessary conditions that will guarantee a repeated or continuous growth of those 5% of the total crack population.

Step 3. Repeated and continuous growth of mechanically short/shallow cracks. The test results shown in Fig. 5 also reveal the reactivated crack growth after dormancy induced by static hold if the test condition after dormancy is adequate to reactivate. It is unlikely that those growing cracks, about 5% of the total population, can grow continuously to the critical size causing pipeline rupture. It would be more plausible to consider that these growing cracks were experiencing repeated cycles of dormancy and active growth. A brief analysis of the operating parameters provides evidence to support the above suggestions. We can take an X-65 pipe with 9.88 mm (0.389") wall thickness as an example. Pipelines are normally operated at a design stress of 0.72 SMYS; 80% of pressure cycles recorded in high-pressure gas transmission line systems have a stress

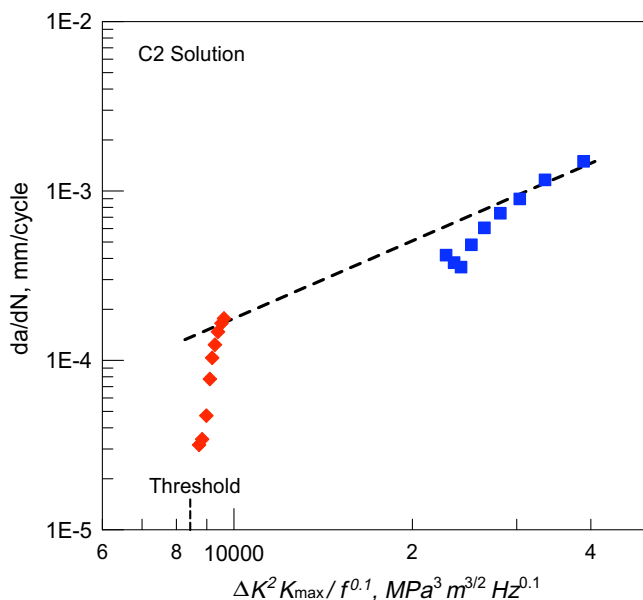


Fig. 13. Crack growth rate (da/dN) as a function of $\Delta K^2 K_{\max}/f^{0.1}$ in C2 solution.

ratio ranging from 0.95 to 1 (static) [42]. The crack is assumed to be 1 mm deep and has a length/depth ratio of 10 (typical for cracks in the field [9]). Since crack colonies are found at the pipe surface with high tensile residual stress, a tensile residual stress of 200 MPa is added to the hoop stress for the calculation of growth rate [21]. Based on the growth equation determined in Ref. [30], a growth rate of $6.9 \times 10^{-13} \text{ mm s}^{-1}$ is obtained at $R = 0.95$ and $f = 1 \times 10^{-5} \text{ Hz}$ (about one cycle per day, typical of high-pressure gas transmission lines). At this growth rate, it would take about 4500 years to grow 0.1 mm, which is basically a dormant state, i.e. approximately 80% of time cracks are in a dormant state. The average growth rate determined in the field is at a magnitude of $10^{-8} \text{ mm s}^{-1}$ ($\sim 0.3 \text{ mm year}^{-1}$) [5–7]. Therefore, growth through repeated dormancy and reactivation is highly plausible.

The above considered steps of crack growth resemble closely the weakest link model proposed for the formation of cleavage crack in steels [56]. This model proposes that there must exist a weakest link for crack initiation and a critical mechanical state acting at the microcrack formed at the weakest link in order to induce propagation after initiation. A similar path of crack initiation and growth after damage to the protective coating, resulting in near-neutral pH groundwater accessing the pipe, is proposed in Fig. 14. The probability of producing those cracks that may experience repeated growth is low unless all the weakest conditions at various stages are met at certain locations on the pipe surface.

The controlling factors for each of the links are also listed in Fig. 14. The first two steps, as discussed above, determine whether crack colonies can be formed on the pipe surface. The third growth step identified above is believed to be related to hydrogen effects in addition to

the usual effects of mechanical driving force, which are further elaborated below.

4.4.2. Role of hydrogen

It is believed that the hydrogen effects, particularly together with the mechanical driving factors, are necessary conditions that could yield repeated crack growth. This suggestion can be understood firstly by examining a crack colony near the rupture site of pipeline steel removed from the field, as shown in Fig. 15.

One unique feature shown in Fig. 15 is the separation of the region with cracks (cracking zone) from the region with corrosion (corrosion zone). In a disbonded holiday as illustrated in Fig. 16, the cracking zone is usually observed in a narrow area within the disbonded coating where ground-water is trapped. It is often believed that cracks develop

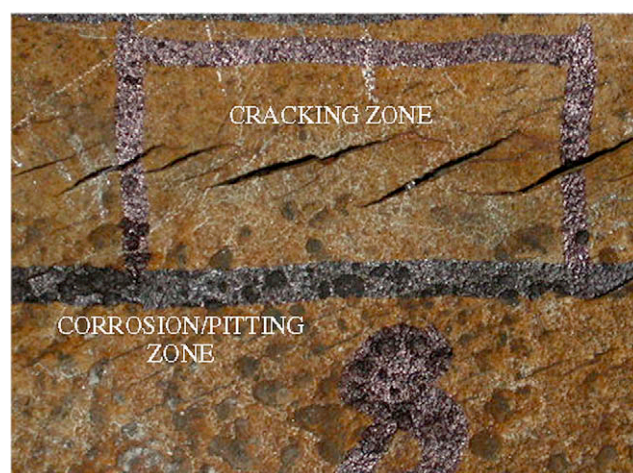


Fig. 15. Near-neutral pH cracks and pitting corrosion found near the site of rupture of a buried pipeline after field service for about 19 years.

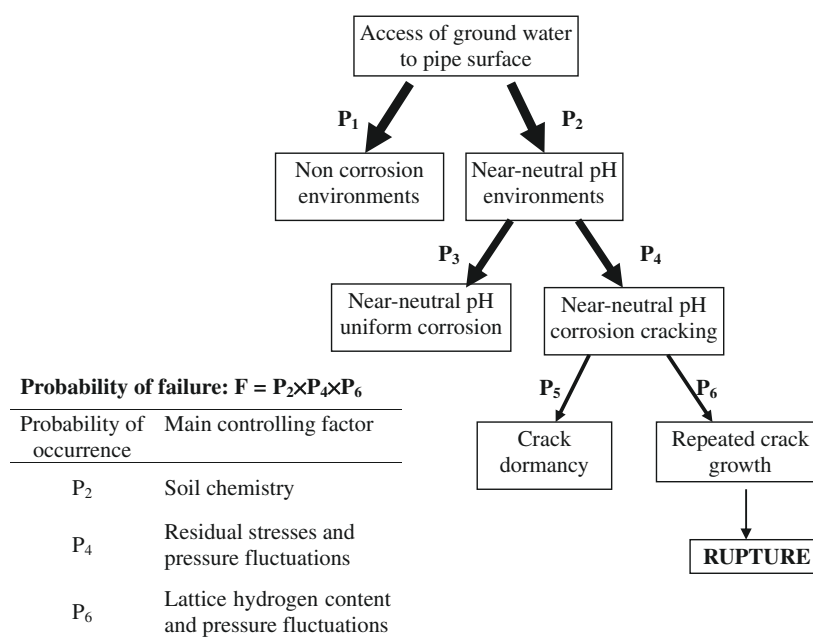


Fig. 14. Schematic illustration showing various events leading to the final rupture of the pipeline steels exposed to near-neutral pH soil environments.

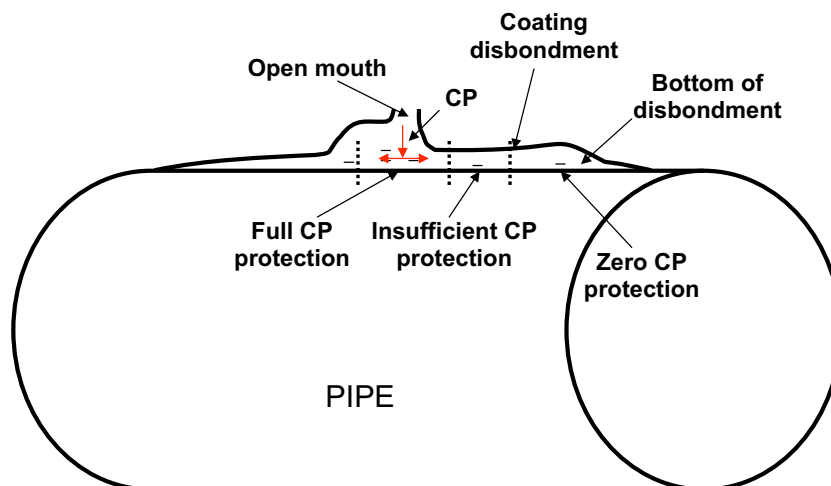


Fig. 16. Schematic showing disbonded coating on pipe surface and reduced cathodic protection toward the bottom of a disbonded holiday.

in the corrosion zone where cathodic protection is completely unavailable, allowing a state of free corrosion to occur. In addition to the cracking zone and the corrosion zone, there is also a protection zone near the opening of the holiday where full cathodic protection can be achieved. Based on the results obtained from this investigation, the unique features shown in Fig. 15 are explained below:

- (1) The fact that little corrosion has taken place in the cracking zone suggests that this zone had been cathodically protected to some extent. Most likely, the cracking zone is partially protected as a full cathodic protection will completely inhibit the occurrence of corrosion and corrosion cracking. A partial cathodic protection prevents the occurrence of general/uniform corrosion but allows corrosion to occur at some localized area, such as the crack tip or specific microstructural features. The corrosion zone adjacent to the cracking zone is characterized with uniform corrosion or shallow corrosion pits due to a state of free corrosion. Due to the presence of cathodic potential, more hydrogen will be generated in the cracking zone than the corrosion zone. This is consistent with the results of hydrogen permeation tests, from which hydrogen content in the steel was found to increase almost linearly with increasing cathodic potential (more negative) [48].
- (2) Even in the absence of some external cathodic current in the cracking zone, a galvanic process may be established between the cracking zone and the corrosion zone, in which the corrosion zone is anodic while the surface of cracking zone is cathodic. The dissolution of Fe at the anode causes corrosion, while electrons generated from Fe dissolution in the corrosion zone are used to reduce hydrogen ions in the cracking zone. Therefore excessive atomic hydrogen relative to the corrosion zone is generated in the cracking zone.

Both these two scenarios have generated more hydrogen in the cracking zone, one of the necessary conditions for the repeated crack growth. The critical role played by hydrogen in terms of repeated growth in the field can also be seen from Fig. 13. The value of $(\Delta K^2 K_{\max}/f^{0.1})$ calculated based on the field operating conditions is normally below or near the threshold determined using CT specimens [49]. Cracks developed in the field are short/shallow cracks and can grow at a $(\Delta K^2 K_{\max}/f^{0.1})$ value below the threshold due to short/shallow crack effects [39–41]. The hydrogen effects become predominant only under low $(\Delta K^2 K_{\max}/f^{0.1})$ loading conditions, as indicated by the results shown in Fig. 13.

There may exist many situations in the field under which lattice hydrogen concentration surrounding the crack tip can be increased. The most influential situation may be related to an increase in cathodic protection. Other situations may include, for example, an increase in water conductivity that may extend the cathodic protection to a wider region and may increase the cathodic potential over the regions with dormant cracks, an increased dissolution rate due to excessive CO_2 in the environments, and of course the soil chemistry and the duration of water exposure. These situations act together with the mechanical driving force (effects of pressure fluctuations) and allow cracks at certain locations to grow repeatedly, possibly at a growth rate at the time of growth much higher than the average growth rate estimated in the field, which is of the order of $10^{-8} \text{ mm s}^{-1}$, owing to the fact that cracks stay dormant over a large portion of time in service as discussed previously.

5. Conclusion

This investigation has provided a comprehensive analysis of possible conditions and their contributions to the crack growth in buried pipeline steels exposed to near-neutral pH aqueous soil solutions. Special attention has been

paid to those cracks, typically 5% of the total crack population, that can propagate continuously or repeatedly and thereby cause the pipe to rupture. The following are the principal conclusions:

- (1) Crack growth in near-neutral pH environments was related to two competitive processes at the crack tip: intrinsic blunting and extrinsic sharpening. The former originates from the low-temperature creep at the crack tip due to either near-static loading or fatigue loading at very low frequency, and active dissolution over the deformed crack tip without passivation of the crack surface. The extrinsic sharpening is governed by the mechanisms of fatigue and the hydrogen effects. The balance of both the intrinsic and extrinsic processes determines whether cracks will be dormant or grow actively.
- (2) Under static loading (conducive to SCC), crack tip blunting is predominant and thus cracks would always stay dormant. When cracks are subjected to cyclic loading (conducive to corrosion fatigue), the blunting process is attenuated but the sharpening process is enhanced such that the two processes can be very comparable depending on variations of service conditions including alteration of environments, cathodic protection and pressure fluctuations.
- (3) Since pipelines, particularly those for high-pressure gas transmission, are operated under a near static condition most of time, crack growth proceeds normally by repeated cycles of dormancy and active growth with a growth rate substantially higher than generally estimated in the field.
- (4) For a given pipeline system, the presence of near-neutral pH environments and high residual stresses on pipe surface determines whether a crack colony can be developed, while the presence of highly diffusible hydrogen at particular locations within some crack colonies is thought to determine whether repeated crack growth can occur. Hydrogen produced by corrosion at the crack tip is secondary in terms of crack growth, as compared with the amount of hydrogen generated from pipeline surface either resulting from general corrosion or cathodic reaction.
- (5) There exist many situations in the field that could enhance the generation of diffusible hydrogen at the pipe surface within a crack colony. This is believed to be a key reason that a small fraction of cracks, typically 5% of the total population, can grow repeatedly to cause pipeline rupture.

Acknowledgments

The authors would like to thank US Department of Transportation, TransCanada Pipelines Limited, Spectra Energy Transmission, Natural Science and Engineering Research Council of Canada for financial support.

References

- [1] Staehle RW, Staehle RW, et al., editors. Stress corrosion cracking and hydrogen embrittlement of iron base alloys, NACE-5. Houston (TX): NACE; 1977. p. 193.
- [2] Jones DA. Principles and prevention of corrosion. 2nd ed. Upper Saddle River (NJ): Prentice Hall; 1996. p. 291.
- [3] Evans JT, Parkins RN. *Acta Metall* 1976;24:511.
- [4] Revie RW, Uhlig HH. Corrosion and corrosion control. New York: John Wiley; 2008. p. 173.
- [5] Parkins RN. A review of stress corrosion cracking of high pressure gas pipelines. In: Proceedings of corrosion 2000. Houston (TX): NACE; 2000. Paper 00363.
- [6] Parkins RN, Blanchard Jr WK, Delanty BS. *Corrosion* 1993;50:395.
- [7] Parkins RN, Blanchard WK, Delanty BS. *Corrosion* 1994;50:394.
- [8] Liu X, Mao X. *Scripta Metall Mater* 1995;33:145.
- [9] Chen W, King F, Vokes ED. *Corrosion* 2002;58:267.
- [10] King F, Given R, Chen W. Detailed characterization of SCC cracks from the Nordegg rupture site and their mechanistic implications. Internal Report #01442. Nova Research & Technology Corp., November 2000.
- [11] Chen W, Bovan GV, Rogge R. *Acta Mater* 2007;55:43–53.
- [12] He D, Jack TR, King F, Chen W. Effect of surface scratch roughness and orientation on SCC of line pipe steel in neutral pH environment. In: 2000 International pipeline conference, vol. 2; 2002. p. 997.
- [13] Elboujdaini M, Wang YZ, Revie RW, Parkins RN, Shehata MT. Stress corrosion crack initiation processes: pitting and microcrack coalescence. In: Proceedings of corrosion 2000. Houston (TX): NACE; 2000. Paper no. 00379.
- [14] Chen W, Wang SH, Chu R, King F, Jack TR, Fessler RR. *Metall Mater Trans* 2003;34A:2601.
- [15] Chu R, Chen W, Wang SH, King F, Jack TR, Fessler RR. *Corrosion* 2004;60(3):275.
- [16] Kushida T, Nose K, Asahi H, Kimura M, Yamane Y, Endo S. et al. Effects of metallurgical factors and test conditions on near-neutral pH SCC of pipeline steels. In: Proceedings of corrosion 2001. Houston (TX): NACE; 2001. Paper no. 01213.
- [17] Wang S, Chen W. *Corrosion* 2002;58(6):526.
- [18] Fang BY, Eadie RL, Chen W, Elboujdaini M. *Corrosion Eng Sci Technol* 2009;44(1):32.
- [19] Fang BY, Eadie RL, Chen W, Elboujdaini M. *Corrosion Eng Sci Technol*; in press. doi:10.1179/147842208X386304.
- [20] Qin Z, Demko B, Noel J, Shoesmith D, King F. *Corrosion* 2004;60(10):906.
- [21] Beavers JA, Johnson JT, Sutherby RL. Materials factors influencing the initiation of near-neutral pH SCC on underground pipelines. In: Proceedings of the 3rd international pipeline conference, vol. 2. Calgary, Canada; 2000. p. 979.
- [22] Bovan GV, Chen W, Rogge R. *Acta Mater* 2007;55:29.
- [23] Lu BT, Luo JL. *Corrosion* 2006;62(8):723.
- [24] Zheng W, Bibby D, Li J, Bowker JT, Gianetto JA, Revie RW, Williams G. Near-neutral pH SCC of two line pipe steels under quasi-static stressing conditions, vol. 2. IPC 2006. p. 95.
- [25] Fang B, Han EH, Wang J, Ke W. *Corrosion* 2007;63:419.
- [26] King F, Jack T, Chen W, Wang SH. In: Proceedings of corrosion 2001. Houston (TX): NACE; 2001. Paper no. 214.
- [27] Sutcliffe JM, Fessler RR, Boyd WK, Parkins RN. *Corrosion* 1972;28:313.
- [28] Meletis EI. *J Mech Behavior Mater* 1996;7:1.
- [29] Leis N, Parkins RN. *Fract Fatigue Eng Mater Struct* 1998;21:583.
- [30] Chen W, Sutherby RL. *Met Mater Trans A* 2007;38A:1260.
- [31] Wang S, Chen W. *Mater Sci Eng* 2002;A325:144.
- [32] Wang S, Zhang YG, Chen W. *J Mater Sci* 2001;36:1931 (8).
- [33] Wang S, Chen W. *Mater Sci Eng A* 2001;A301:147.
- [34] Zhao J, Mo T, Nie DF, Ren M, Guo X, Chen W. *J Mater Sci* 2006;41:6431.

- [35] Sofronis P, McMeeking RM. *J Mech Phys Solids* 1989;37(3):317.
- [36] Troiano AR. The role of hydrogen and other interstitials in the mechanical behavior of metals (1959 Edward De Mille Campbell Memorial Lecture). *Trans ASM* 1960;52:89.
- [37] Gangloff RP. Hydrogen-assisted cracking in high-strength alloys. *Comprehensive structural integrity: environmentally-assisted fracture*, vol. 6. Oxford: Elsevier; 2003.
- [38] Uhlig HH, Rhodin TN, editors. *Physical metallurgy of stress corrosion fracture*. New York: Interscience; 1959. p. 1.
- [39] Chen W, Kania R, Worthingham R, Kariyawasam S. Crack growth model of pipeline steels in near-neutral pH soil environments. In: *International pipeline conference*. Calgary; 2008. Paper no. IPC08 64475.
- [40] Torng TY, McClung RC. Probabilistic fatigue life prediction methods for small and large fatigue cracks. In: *Proceedings of the 35th structures, structural dynamics, and materials conference*; 1994. p. 1514.
- [41] McClung RC, Sehitoglu H. *ASME J Eng Mater Technol* 1992;114:1.
- [42] Wang SH, Chen W, King F, Jack TR, Fessler RR. *Corrosion* 2002;56(6):526.
- [43] Wang YZ, Revie RW, Shehata MT. In: Collins L, editor. *Materials for resource recovery and transport*. The Metallurgical Society of CIM; 1998. p. 71.
- [44] Chen W, Eadie RL, Sutherby RL. Environmental effects on near-neutral pH stress corrosion cracking in pipelines. In: *Second international conference on environment-induced cracking of metals*. Banff, Alberta, Canada: The Banff Centre; 2004.
- [45] Chen W, Sutherby R. Laboratory simulation of hydrostatic test in near-neutral pH soil environments. In: *International pipeline conference*; 2006. Paper no. IPC06 10477.
- [46] Qiao L, Mao X. *Acta Metall Mater* 1995;43:4001.
- [47] Lu BT, Luo JL, Norton PR, Ma HY. *Acta Mater* 2009;57(1):41.
- [48] Chen W, Wilmott ML, Jack TR. Hydrogen permeation behaviour of X-70 pipeline steel in NS4 neutral pH environment. In: *International pipeline conference*, vol. 2; 2000. p. 953.
- [49] He DX, Chen W, Luo JL. *Corrosion* 2004;60(8):778.
- [50] Anderson TL. *Fracture mechanics fundamentals and applications*. 3rd ed. Boca Raton, FL: CRC Press; 2005. p. 234.
- [51] Lynch SP. *Acta Metall* 1988;36:2639.
- [52] Niburab KA, Bahra DF, Somerdayb BP. *Acta Mater* 2006;54:2677.
- [53] Uyama H, Nakashima M, Morishige K, Mine Y, Murakami Y. *Fatigue Fract Eng Mater Struct* 2006;29:1066.
- [54] Hörlund E, Fossen JKT, Hauger S, Haugen C, Havn T, Hemmingen T. *Int J Electrochem. Sci* 2007;2:82.
- [55] Anderson TL. *Fracture mechanics, fundamentals and applications*. 3rd ed. Boca Raton (FL): CRC Press; 2005. p. 488.
- [56] Anderson TL, Stienstra DIA, Dodds RH Jr. A theoretical framework for addressing fracture in the ductile–brittle transition region. In: *Fracture mechanics: 24th Volume. ASTM STP 1207*. Philadelphia, PA: American Society for Testing and Materials; 1994.

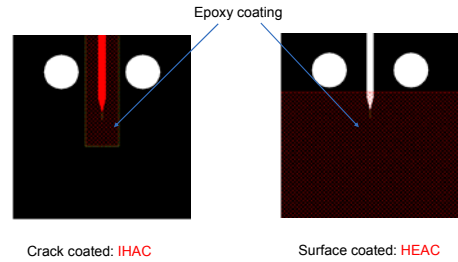


Simulation of Crack Growth in Hydrostatic Testing

Yongwang Kang

Department of Chemical and Materials Engineering, University of Alberta

Sample design



Crack coated: IHAC

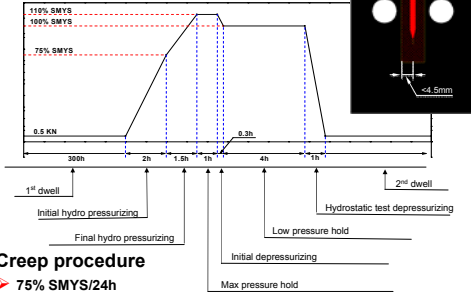
Surface coated: HEAC

2 Department of Chemical and Materials Engineering

University of Alberta

Procedure

❖ Loading procedure



❖ Creep procedure

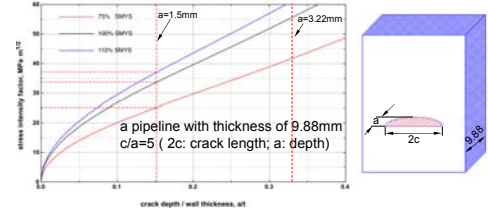
➤ 75% SMYS/24h

3 Department of Chemical and Materials Engineering

University of Alberta

Hypothesis and Testing Condition

❖ Hypothesis



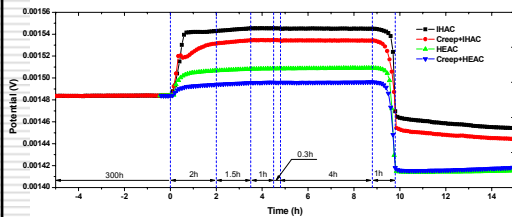
❖ Test condition

- X65 (Spectra Energy Transmission)
- C2 solution
- 5% CO₂+N₂ purging

4 Department of Chemical and Materials Engineering

University of Alberta

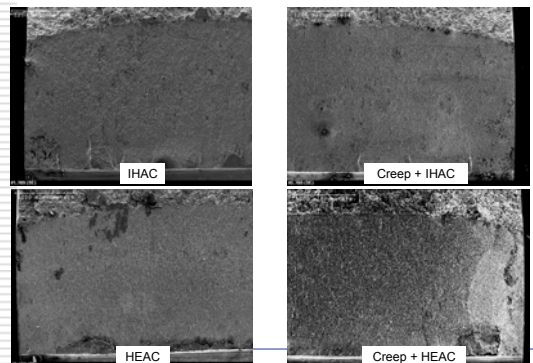
Potential change (a=1.5mm)



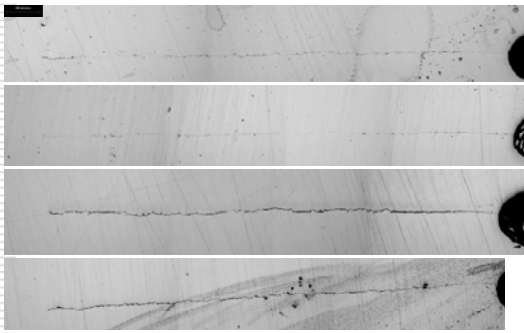
Department of Chemical and Materials Engineering

University of Alberta

Microstructure of crack surface



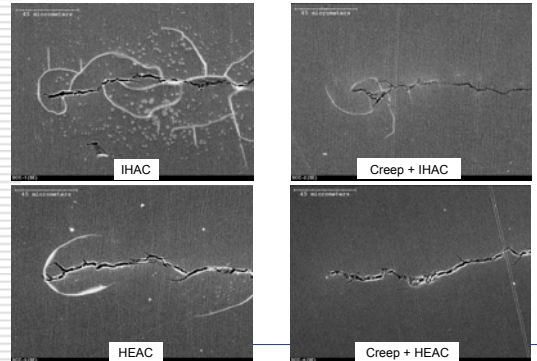
Width of crack



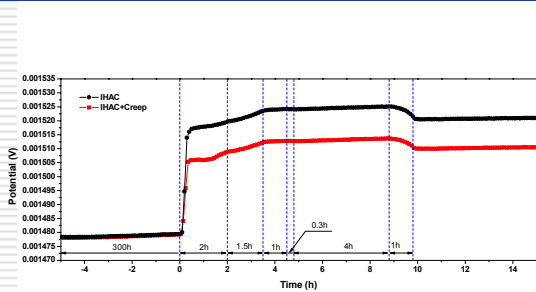
Department of Chemical and Materials Engineering

University of Alberta

Microstructure of crack tip

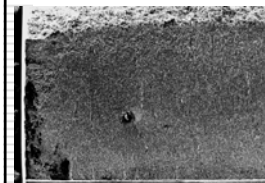


Potential change ($a=3.22\text{mm}$)

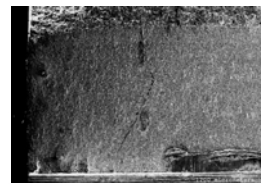


Department of Chemical and Materials Engineering

University of Alberta



IHAC

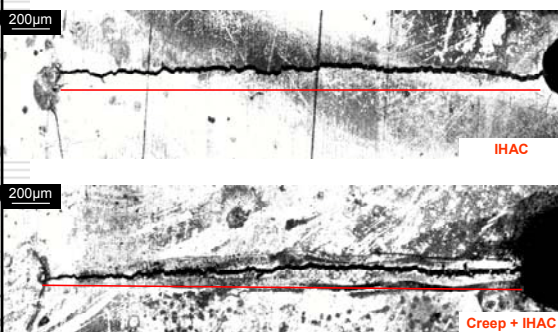


Creep + IHAC

Department of Chemical and Materials Engineering

University of Alberta

Length of crack

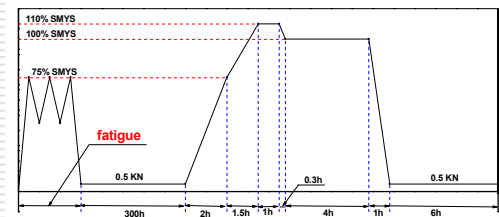


Department of Chemical and Materials Engineering

University of Alberta

Future work

- ❖ Testing the sample with assuming crack depth of 3.22mm in the hydrogen-environment-assisted condition
- ❖ Effect of fatigue



Department of Chemical and Materials Engineering

University of Alberta

Growth of surface stress corrosion cracks in near neutral pH environments under disbonded coatings

By: Afolabi Egbewande

Near neutral pH SCC

- Near neutral pH SCC is an important problem in the oil/gas industry
- A lot is yet to be well understood about crack growth behaviour
- Current model yields poor correlation for NNPHSCC

Crack growth models

- Superposition model

$$\left(\frac{da}{dN}\right)_{total} = \left(\frac{da}{dN}\right)_{fatigue} + \frac{1}{f} \left(\frac{da}{dt}\right)_{SCC}$$

- Crack tip strain rate

$$\dot{\epsilon} \approx 4f(1-R)$$

Both models have yielded poor correlation with NNPHSCC crack growth

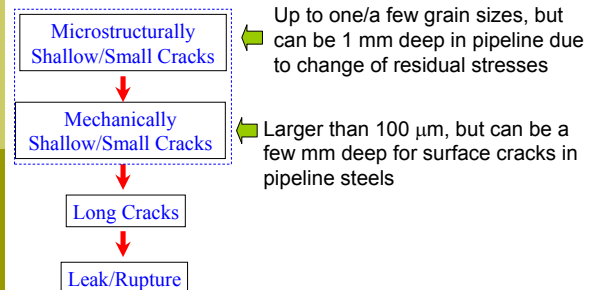
- True corrosion fatigue model

$$\left(\frac{da}{dN}\right) = \Delta K^2 K_{max} / f^\alpha$$

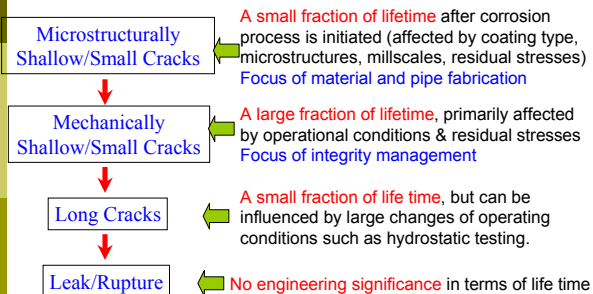
All three models use a CT specimen & assumed long cracks.

NNPH CRACK GROWTH BEHAVIOR

What are dimensional limits for shallow/short cracks and long cracks in pipeline steels?



NNPH CRACK GROWTH BEHAVIOR



Objective

To develop crack growth model for small/shallow cracks (predicting growth by crack coalescence) that accounts for, environment, mechanical, and metallurgical effects

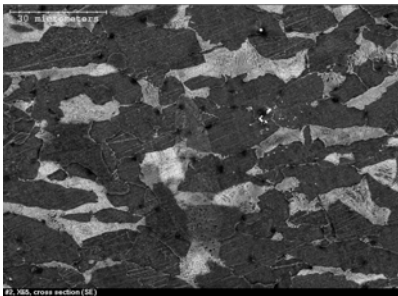
Factors to study

- Applied load and loading parameters
- pH
- Applied cathodic protection current
- Coating disbondment

Research Schedule

- Produce appropriate test samples/test cell
- Design experiments to study growth rate w.r.t. to the effect of:
 - Cyclic load parameters
 - Environmental factors: pH, cathodic protection
- Determine crack growth mechanism
- Produce model predicting mechanism (including crack coalescence)

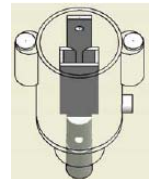
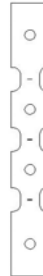
Material



Microstructure of X65(SPECTRA)

Progress

- Sample designed and fabricated
- Test cell designed and fabricated

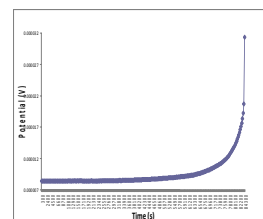


- One test already completed

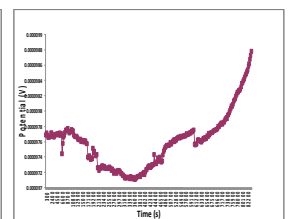
Experimental

- Samples pre-cracked in air.
- Pre-crack crack size $\approx 0.5\text{mm}$.
- $\sigma_{\text{max}} = 100\%\text{SMYS}$
- Cyclic loading frequency = 0.005Hz
- Stress ratio = 0.89 and 0.4
- Crack growth monitored by potential drop system

Progress (cont'd)

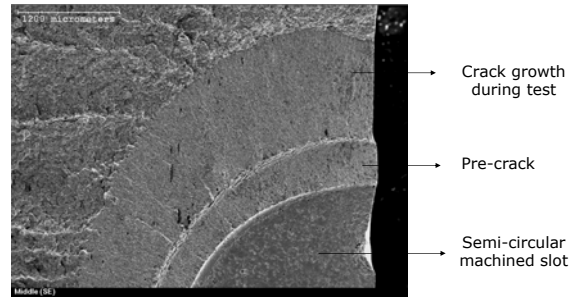
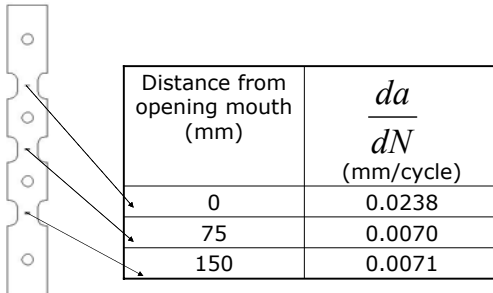


Opening mouth

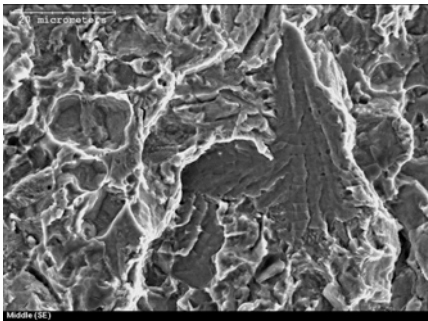


75mm from opening mouth

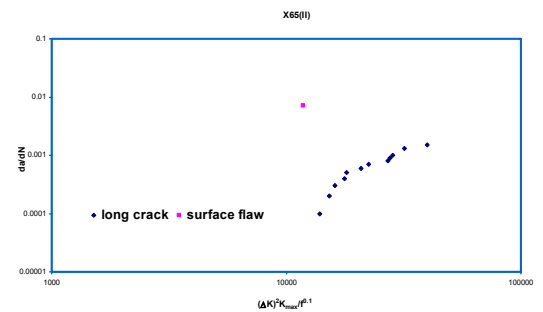
Progress (cont'd)



Crack propagation during cyclic loading in NNPHSCC environment



High magnification image of crack propagation



Comparison of growth rate of long cracks and shallow cracks

Further work

- Determine the effect of loading parameters – R, f, ΔK etc on growth rate.
- Determine the effect of pH variation on growth rate.
- Determine the effect of variation in level of cathodic protection on growth rate.

Summary

- There is a need for a model that adequately predicts crack growth in a NNPHSCC environment.
- The proposed research will yield such a model.

Crack Growth Behavior of Pipeline Steels In Near-Neutral pH Environment

Mohammad Hassan Marvasti

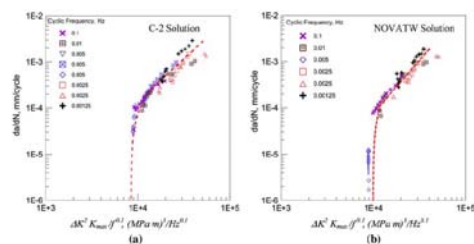
Crack Growth Modeling

- Important factors:
 - ✓ Eunicic Cyclic loading (Fatigue)
 - ✓ Corrosion (Hydrogen)

- Corrosion fatigue:

$$\frac{(\Delta K)^2 K_{\max}}{f^\alpha} \rightarrow \begin{matrix} (\Delta K)^2 K_{\max} \\ \frac{1}{f^\alpha} \end{matrix}$$

Crack Growth Modeling



Crack growth rate da/dN as a function of $\Delta K^2 K_{\max} / f^{0.5}$ obtained from testing in (a) C-2 solution and (b) NOVATW solution.

Research Objective

- Investigate the crack growth behavior (rate) of different pipeline steels using the new corrosion fatigue growth model.
- Find the relation between growth rates and steel properties (microstructures, mechanical Properties).

Materials

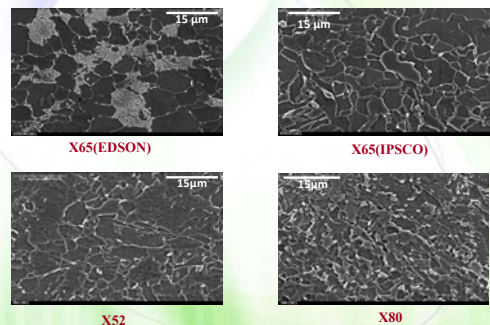
Steel	C	Mn	Cu	Nb	Cr	Mo	V	Ni	Al	Ti	N
X80	0.06	1.75	0.27	0.31	0.04	0.03	0.005	0.08	0.026	0.011	0.003
X65(EDSON)	0.13	1.55	0.05	0.05	0.08	0.01	0.002	0.05	0.042	0.002	0.009
X65(IPSCO)	0.03	1.49	0.27	0.06	0.08	0.21	0.003	0.01	0.001	0.001	0.012
X52	0.07	0.80	0.28	0.09	0.05	0.01	0.002	0.01	0.031	0.019	0.001

*P=0.01, B=0.0002, Si=0.3, S<0.01 and Ca<0.003 for all steels.

Steel	Yield Strength (MPa)	Tensile Strength (MPa)	Total Elongation (%)
X80	619.5	705.1	20.6
X65(EDSON)	522.8	607.8	24.3
X65(IPSCO)	450.7	544.6	30.1
X52	382.2	485.3	32.2

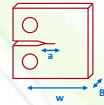
Microstructures

2000X



Experiments

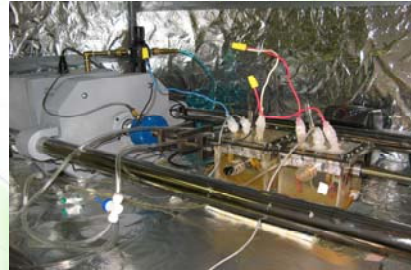
- Precracked CT specimens
- C2 Solution (pH=6.2)
- Pneumatic cyclic loading frame
- Crack growth data
(potential drop test method)
- da/dN vs. $(\Delta K)^2 K_{max}/f^a$ curves.



$$K_{max} = \frac{P_{max}}{B\sqrt{w}} f(a/w)$$

$$\Delta K = \frac{\Delta P}{B\sqrt{w}} f(a/w)$$

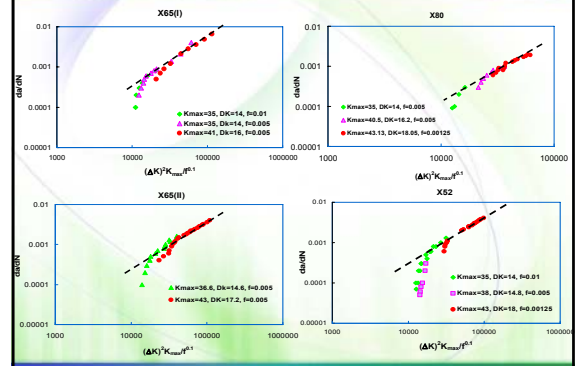
Test Set Up



Experiments

- Ten successful tests including all steels
- $K_{max} = 35-43 \text{ MPa}\sqrt{m}$
 $\Delta K = 14-18 \text{ MPa}\sqrt{m}$
- Triangle Waveform ($f = 0.00125-0.01 \text{ Hz}$)
- Time = 18-60 days (Rupture)

New Materials



New Materials

X80 & X52

Test 1

$K_{max} = 43$

$\Delta K = 18$

$f = 0.00125$

$R = 0.58$

$\Delta K^2 K_{max}/f^{0.1} = 27200$

Test 2

$K_{max} = 35$

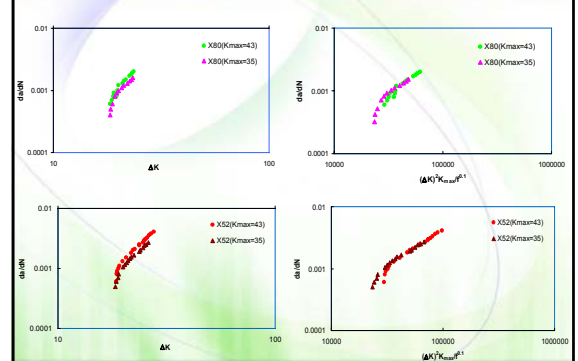
$\Delta K = 18$

$f = 0.00125$

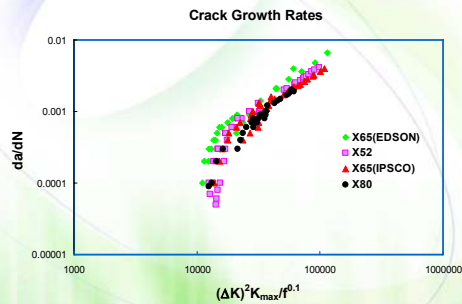
$R = 0.48$

$\Delta K^2 K_{max}/f^{0.1} = 22300$

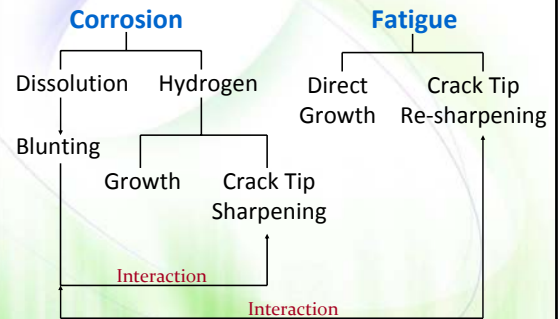
Combined Factor



Corrosion Fatigue



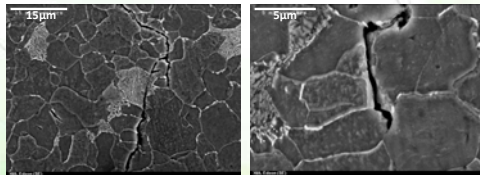
Corrosion Fatigue



X65(EDSON) has the highest crack growth rate:

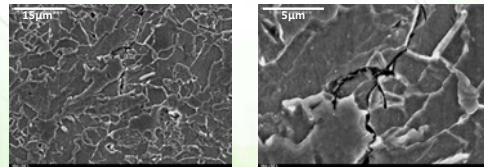
Ferrite/Pearlite interface:

- ✓ Enhanced local corrosion (galvanic cells)
- ✓ Local microscopic plastic deformations
- ✓ High hydrogen trapping ability



X52 has lower crack growth rate:

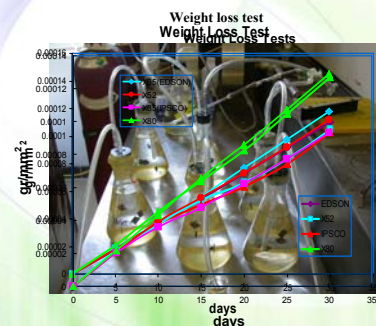
- ✓ Low yield strength
- ✓ Coarse grains (less grain boundary area)
- ✓ Crack tip branching (high fracture toughness)



Corrosion Fatigue

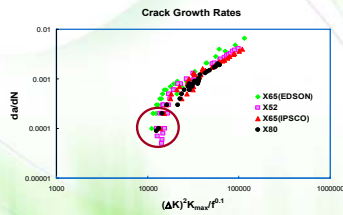
- ✓ Coupon Weight Loss Tests
- ✓ Fatigue resistance of steels
- ✓ Fracture toughness measurement (JIC)

Corrosion

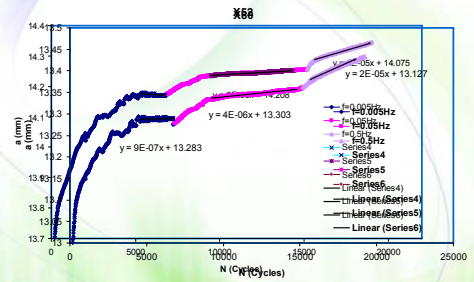


Fatigue (Air)

$$(\Delta K)^2 K_{\max} / f^\alpha \longrightarrow (\Delta K)^2 K_{\max}$$



Fatigue (Air)



Fatigue (Air)

- ✓ Critical Frequency
- ✓ Creep (Crack Tip Blunting)
- ✓ Hydrogen (Crack Tip Re-sharpener)

Future Work

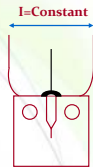
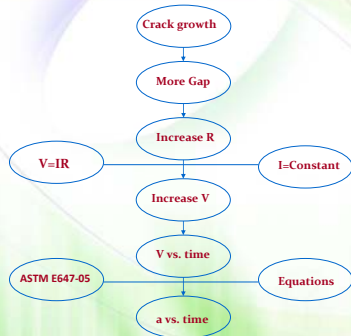
- ✓ Fatigue (Air)
- ✓ Fracture Toughness Tests (J_{IC})

Conclusions

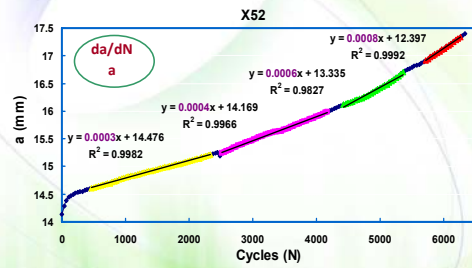
- Crack growth behavior in NNPH environments:
 - ✓ Consistent with corrosion fatigue cracking
 - ✓ Well explained by New Model
 - ✓ Microstructure dependent
- Fatigue Crack Growth is frequency dependent.

Thank You For Your Attention !

Potential Drop Test Method



Crack Growth measurement



Data Analysis

